MRR74 - 02

TECHNICAL REPORT

MF FC AD MM TE IQ MS MR EM CM

INDEX TERMS

Gaging

Machine Tools

Machining

POROUS GRAPHITE AIR-BEARING COMPONENTS AS APPLIED TO MACHINE TOOLS

By

W. H. Rasnick
Development Engineer

T. A. Arehart
Machining General Foreman

D. E. Littleton
Machining Foreman

P. J. Steger
Section Head - Metrology & Precision Machining
Union Carbide Corporation

ABSTRACT

Considerable work has been done at the Oak Ridge Y-12 Plant on the application of porous-graphite restricted, externally pressurized air bearings to machine tool and gaging. This report is primarily a compilation and reorganization of data which will facilitate utilization of the air-bearing technology by manufacturing engineers with little or not previous background in the subject matter.

1974

SOCIETY OF MANUFACTURING ENGINEERS
20501 FORD ROAD
DEARBORN
MICHIGAN, 48128

Creative Manufacturing Engineering Programs

DISCLAIMER

ABSTRACT

Considerable work has been done at the Oak Ridge Y-12 Plant on the application of porous-graphite, restricted, externally pressurized air bearings to machine tool and gaging components. These components have been successfully applied to upgrade machine tool accuracy, provide specialized performance, and to improve gaging processes.

This work was done over a period of several years with continual modification in fabrication technique. As a result, pertinent information is dispersed through various technical writeups. This report is primarily a compilation and reorganization of data which will facilitate utilization of the air-bearing technology by manufacturing engineers with little or no previous background in the subject matter. Material has also been updated where applicable. Although all major applications are covered, the spherical-zone spindle is given special consideration because of its importance and widespread use.

INTRODUCTION

An increasing demand for accuracy in both manufacturing and inspection has led to investigations of externally pressurized air bearings as a means of obtaining an improved bearing system. The externally pressurized air bearing offers many advantages for improved performance of machine tools and inspection machines. Zero starting friction and predictable operating friction with an absence of wear are characteristics attractive for slides and rams. Negligible heat generation at normal machine tool spindle speeds results in good thermal stability of the important spindle-part contour reference planes. Freedom from vibration due to film-averaging effects and improvement in motion accuracy are attractive characteristics when considering special tooling applications and materials such as ceramic or diamond, or very precise inspection requirements. Cleanliness alone may be sufficient justification when considering inspection or special manufacturing processes.

The viscosity of air changes only slightly with temperature; thus, steady performance can be realized over a broad range of temperatures. In addition, the thin pressurized operating film helps prevent bearing contamination from external environmental conditions. Satisfactory bearing applications are thus possible in unusual operating conditions without the need for special seals or operating precautions.

In order to provide a balanced picture, some disadvantages inherent in the use of pressurized air bearings must be mentioned. The principal disadvantage is their relatively poor behavior in the presence of large dynamic force components, which is due to the small inherent damping in the air film. While recent work has shown that the damping coefficient of an air bearing can be maximized by correct design, the values achieved are always likely to be small compared with those of the hydrostatic oil bearing which is therefore rightly preferred for many heavy-duty machine-tool applications.

Another point sometimes raised as an objection to the use of air bearings in an industrial environment is the need for a supply of clean, dry, compressed air and its cost. It is true that in

many firms the compressed air supply is of poor quality with a large water, oil, and dirt content. The short-term answer to this lies in the use of good-quality filters and water separators or, if this is still inadequate, in providing for a small rotary air compressor attached to the machine tool or inspection equipment. In the long term, however, it may well be less expensive to improve the quality of the factory air supply by the installation of better-quality compressors (possibly of the oil-free type) and air dryers; and, most important, by proper maintenance. This latter factor will, in many installations, also reduce air flows due to leaks in factory lines to an extent far outweighing the commonly small air-flow requirements of the air bearings in use.

All of the following comments will be based on experience with porous graphite air bearings. Although not the only type used in the Oak Ridge Y-12 Plant,[a] they are the prevalent type and the type which the authors feel offers the most promising and reliable operation of any type now available for most applications.

POROUS GRAPHITE AIR-BEARING COMPONENTS

APPLICATIONS

Applications for air bearings in machine tools and inspection machines are numerous and can best be divided into the following categories:

1. Rotary-motion applications such as spindles and rotary tables.

2. Linear-motion applications where only positioning of the slide component is carried out on the air film, while actual machining or inspection takes place with the air cut off and the slide clamped.

3. Linear-motion applications where machining or inspection is carried out on a fully pressurized air film.

The most widely used component in Y-12 is the spherical-zone spindle shown in Figure 1. The spindle consists of a basic steel shaft with two hemispherical-segment bearing journals, supported in the bearing housing pads by an externally pressurized air film. The front segment is rigidly fixed to the steel shaft; the rear segment is attached to the shaft through a flexure ring. This ring is prestressed an amount equal to the force exerted by the film pressure acting over its area. It provides a means of bearing-journal position adjustment in the axial direction and at the same time takes up axial expansion of the shaft due to temperature changes during operation. This prestressed ring limits the forward movement of the spindle face to the expansion of that part of the shaft which extends forward from approximately the center of the front bearing. In addition, there is some forward movement due to an increase in thickness of a portion of the front-bearing film as the deflection of the flexure ring changes to take up shaft expansion. Radial clearance in the bearing films is obtained from a combination of the axial adjustment of the rear flexure ring, expansion of the housing due to film pressure, and the spherical radial difference which exists between the shaft journal and carbon bearing.

(a) Operated by the Union Carbide Corporation's Nuclear Division for the US Atomic Energy Commission.

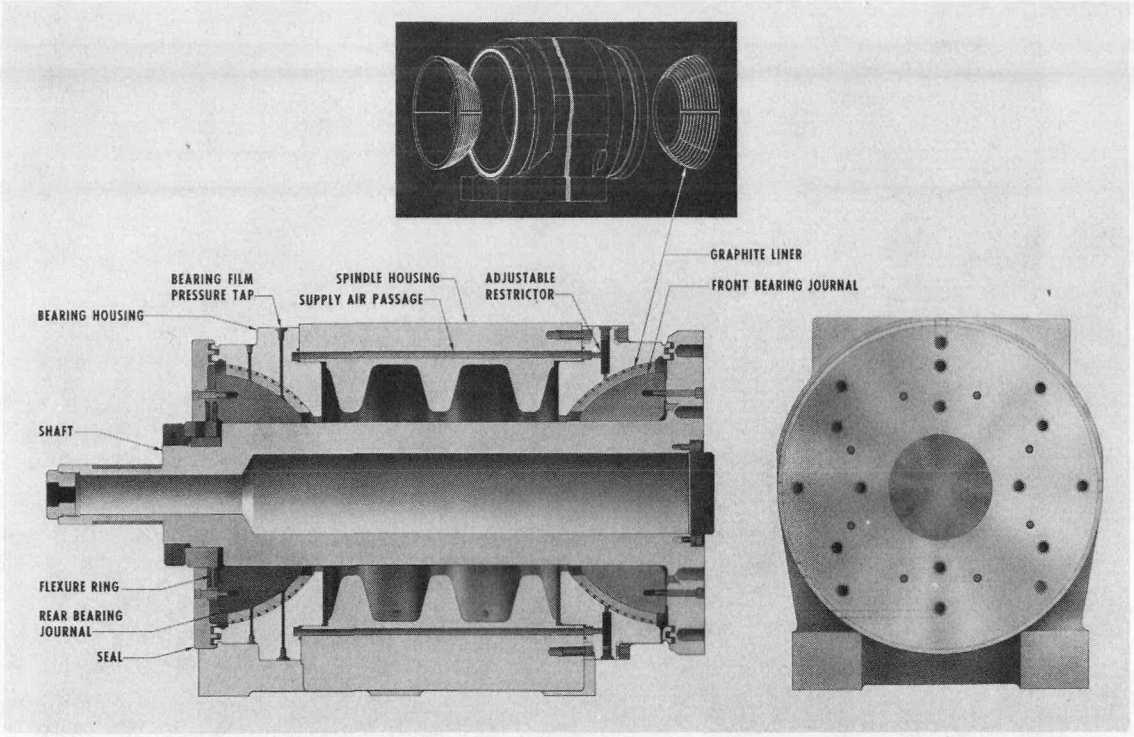

Figure 1. AIR BEARING SPINDLE. (With Spherical-Zone Spindle)

Spindle performance measurements indicated rotational accuracies of 12 microinches (0.304 μm) TIR or less, deflection-load characteristics of less than 1.5 microinches per pound (8.5 nm/N), and a bearing housing temperature rise of less than 2^{o} F (1.1^{o} C) from a cold start to steady-state conditions at a speed of 1000 rpm for the 6-inch (153-mm)-radius size.

Another significant example of rotary air-bearing application was made to a machine-tool steady rest. A type of conventional steady rest used in machining applications consists of rollers supported on ball bearings which are lubricated with grease or oil and cooled with a cutting fluid. While this arrangement is generally satisfactory for low-speed machining operations, problems arise as the surface speed of the workpiece increases due to significant heat generation, roller vibration, and chip fouling. If the roller-bearing assemblies are kept clean and the bearings properly lubricated, little difficulty is encountered at normal machining speeds. Too frequently, however, the lubrication system fails, resulting in bearing deterioration which damages the steady rest and/or machining fixture.

Two types of air-bearing steady rests have been used successfully. The first type is a noncaptive, adjustable-pad arrangement with graphite liners and a spherical seat support; the second type is a captive system consisting of four equally spaced and adjustable pads supported by spherical seats (Figure 2). These steady rests eliminated chip fouling, which was a problem with the roller-bearing steady rests. In suitable production applications, surface speeds have been used that are as high as 4000 feet per minute (20.3 m/sec) at the bearing film. Some maintenance has been required on a routine basis. While cutting fluids and chips have not been a problem, it seems that after four to six months of operation, permeability is reduced. This problem apparently stems from fluid contamination, and the graphite-bearing pad needs to be flushed clean. This operation can easily be performed in eight hours. In general, where higher surface speeds are necessary, the air-bearing steady rest provides a significant performance improvement over the roller-bearing steady rest.

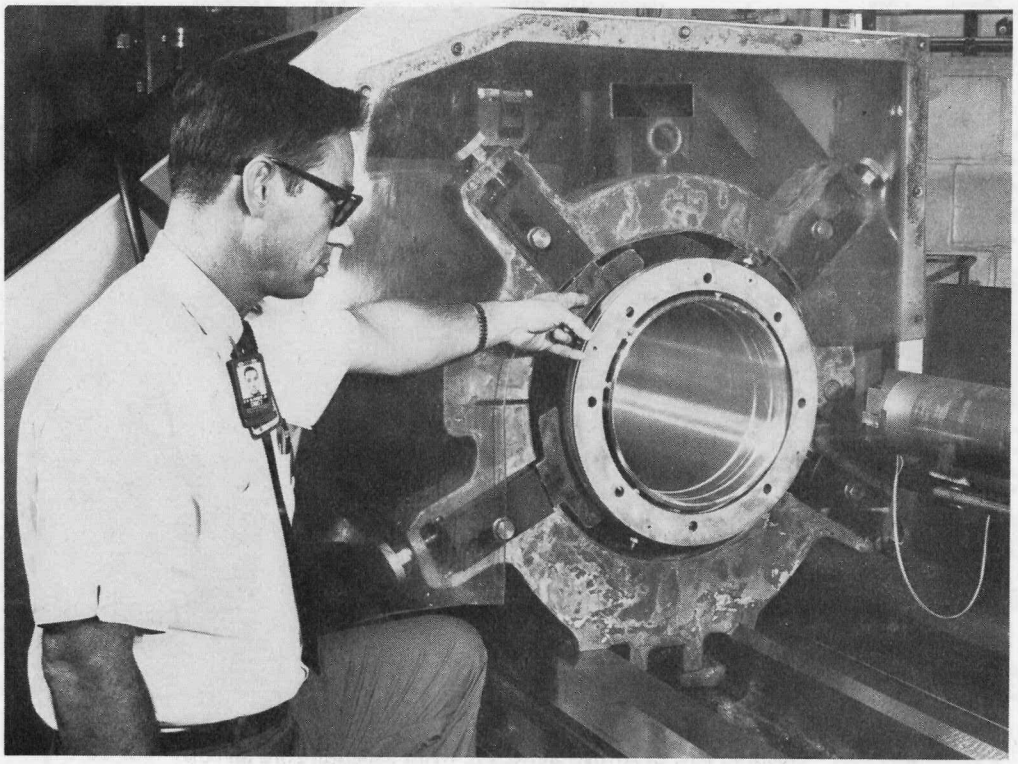

131628

Figure 2. AIR BEARING STEADY REST - CAPTIVE DESIGN.

Several significant linear-motion air-bearing applications have been made for continuous machining and inspection use. One of the more significant applications has been the use of the linear-motion ram, shown in Figure 3, to provide a third improved axis of measurement capability to a precision jig borer having 30 inches (0.763 m) of travel with a laser interferometer measuring system. Flexibility and ease of fabrication are prime advantages of the design (Figure 4). The small pads are easily lapped to a flatness of 10 microinches (0.254 μm). The spherical seat provides automatic alignment of the bearing pad to the ram, and the adjustment-screw arrangement allows microinch film clearance without the costly fabrication of microinch tolerances. In addition, maintenance is simplified since the pad is removable without disassembly of the housing. Ram travel over 30 inches (762 mm) was straight within 50 microinches (1.27 μm) in one plane and 75 microinches (1.9 μm) in the other plane. The measuring accuracy over the 30 inches (762 mm) of travel was ± 75 microinches (± 1.9 μm).

With the development of the graphite impregnation technique, noncaptive air bearings are now feasible for large-mass, small-force applications such as encountered in some machining and many inspection applications. Two such applications were recently made to a tape-controlled turning and boring machine tool, shown in Figures 5 and 6, by replacing the roller bearings with both self-aligning and fixed-air-bearing pads. A view of the self-aligning pads is presented in Figure 7. Both systems have been evaluated and are presently being used in normal machine operations.

Results of the evaluation studies of the slide made to date indicate good stability during operation for a range of tool moments over the entire range of its capacity. In this case, the slide is limited by design to 2000 inch pounds (226 Nm) of moment due, primarily, to the fact that limitations in the support area came about in adapting the system from the original roller-bearing

concept. Static compliance agreed well with calculations after corrections were made to account for bearing distortion and geometry errors for the fixed system. Very little correction was needed for the self-aligning system. Another advantage in this design was in reduced fabrication tolerance and ease of installation.

There are several advantages in the use of air bearings for this application. Present machines have oil-lubricated roller bearings. Roller bearings require precision surfaces on both sides of the rollers to obtain slide accuracy. Air bearings eliminate the need for one of the precision surfaces. Short-wavelength variations are averaged by the film; long wavelengths remain constant through use and could be easily corrected for using cam compensation. Maintenance due to impact load damage to the rollers and/or ways is eliminated through the cushioning effect of the air film (viscous damping) and the large area of support. Slide stiffness and load capacity can be maintained with the present 90-psig (620-kPa) air supply through effective design of the bearing pads and support system. Thin operating films are required for stiffness and sufficient film area for load capacity.

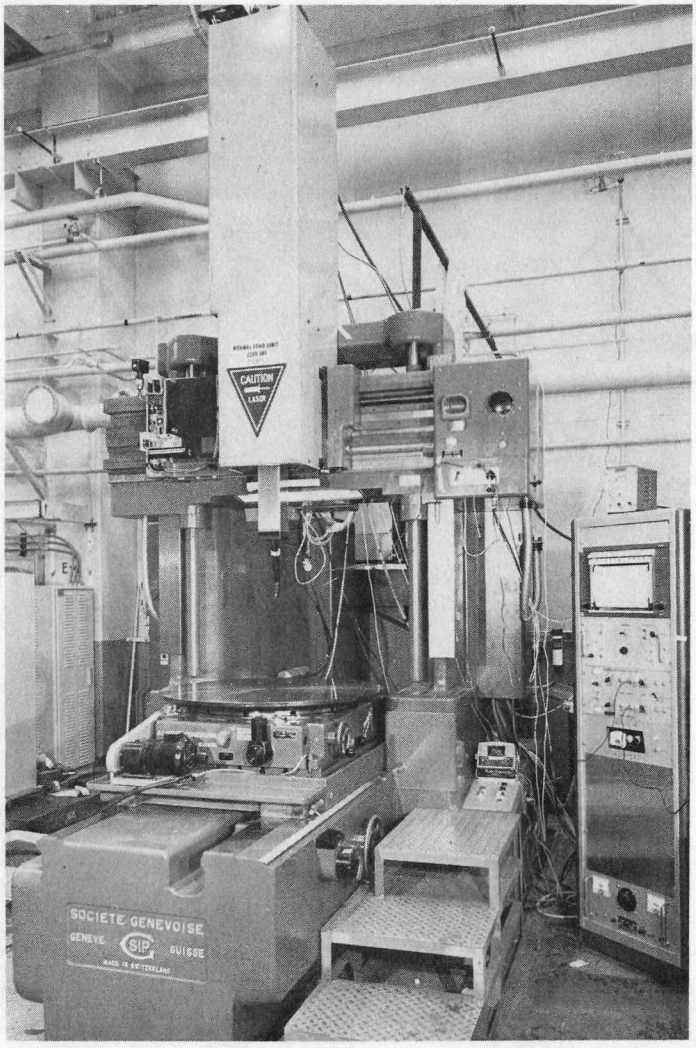

132305

Figure 3. AIR BEARING RAM ON MEASURING MACHINE.

Many specialized applications of air bearings in the inspection field have been made: (1) a small spherical bearing (see Figure 8) to measure the deviation of mass center to geometry center within 100 microinches (2.54 μm) of 4-inch (102-mm) solid tungsten spheres; (2) long-range, air-bearing-supported linear voltage differential transformers (LVDT) and laser gages; (3) segmented bearings for rotating a transducer about a point; (4) self-aligning fixtures using air to support the part, and (5) gaging fixtures which are both supported and positioned on an air film. A recent development is an improved-performance, standard-range LVDT (see Figure 9). The standard LVDT, as used extensively in dimensional inspection applications, is limited in most instances by the close-clearance linear sleeve bearing between the shaft and housing. In certain areas of operation, fine particulates and vapor contamination collect between the shaft and linear bearing. As a result, the shaft sticks in the bearing and erratic coefficients of friction develop. Also, linear movement of the gaging tip becomes difficult. To overcome these difficulties and provide increased operational reliability, higher gaging forces are employed for dimensional measurements. Sometimes, the higher forces required for linear movement of the gaging tip can cause damage to the surface finish of articles being measured. Also, the higher

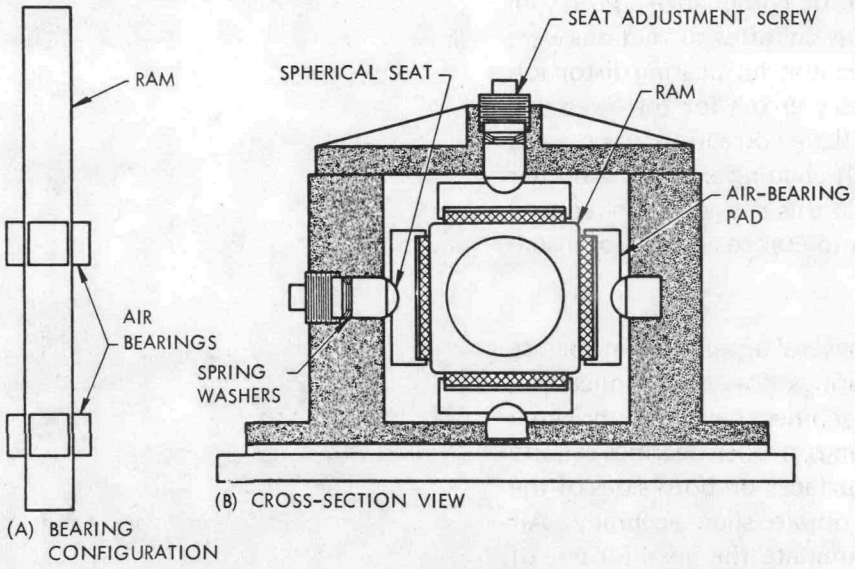

Figure 4. CROSS SECTION OF AIR BEARING RAM.

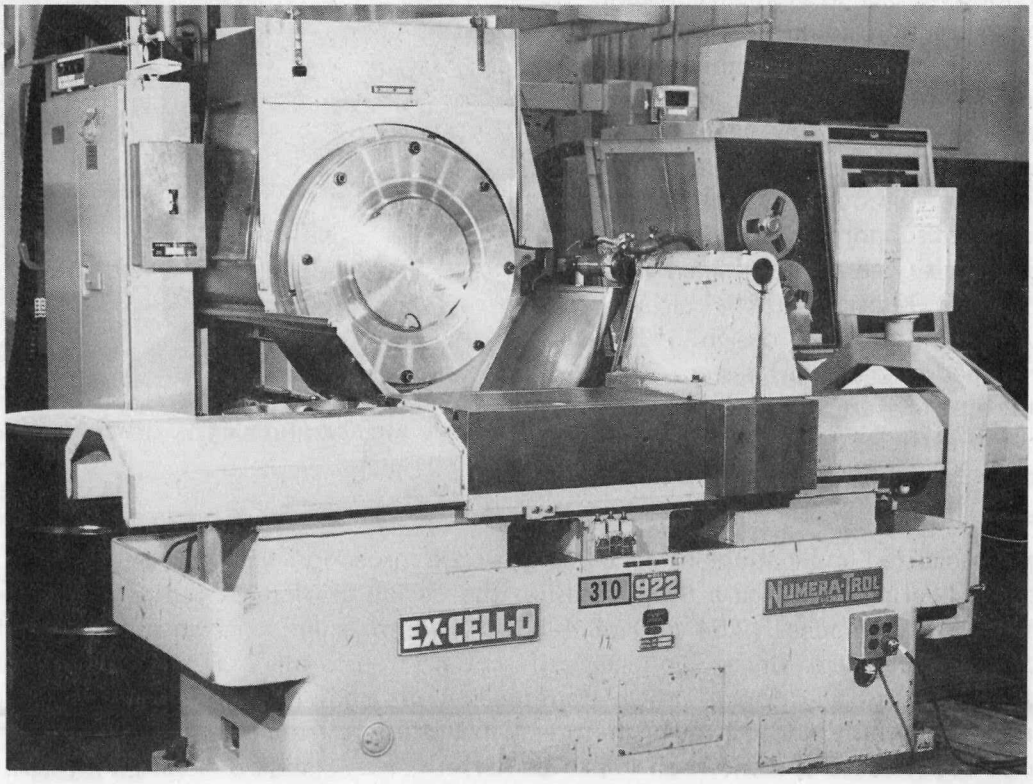

141085

Figure 5. MACHINE TOOL WITH AIR BEARING SLIDE.

forces can result in side deflection of the gaging tip to cause significant errors in dimensional measurements. The LVDT with air bearings eliminates these unwanted friction-associated performance parameters while improving reliability and accuracy. In addition, it is possible to reduce gaging forces to as low as two grams (0.02 N) when used in the horizontal position compared to the standard gaging force of 50 grams (0.490 N) and higher.

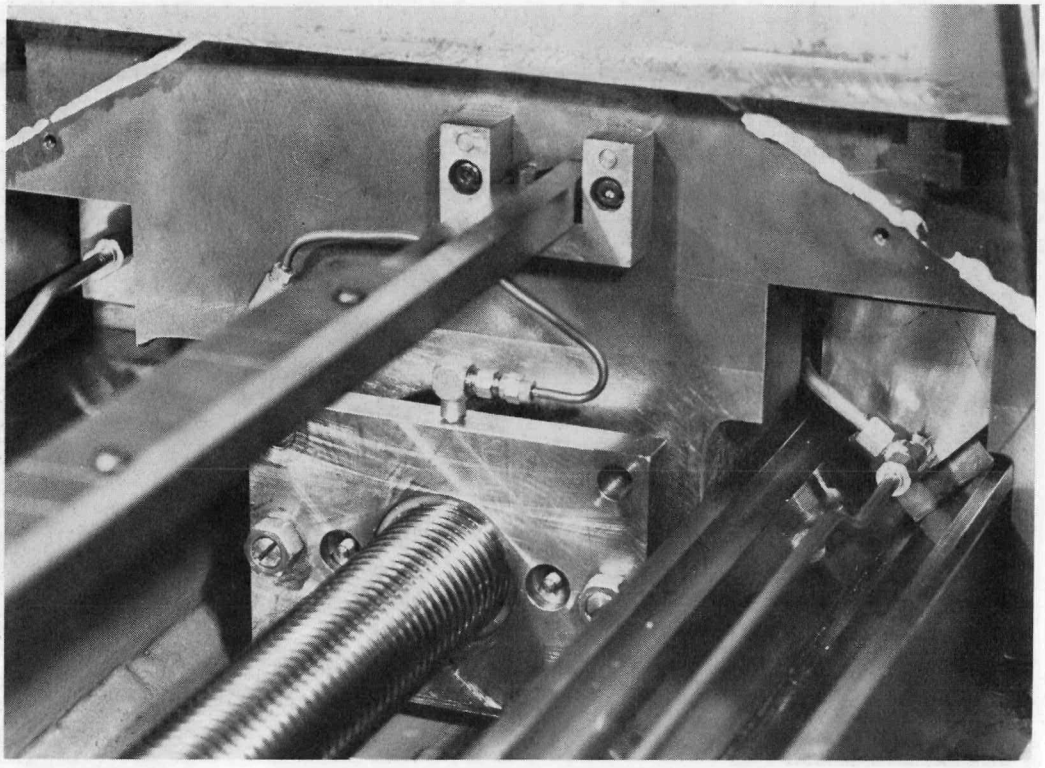

141086

Figure 6. CLOSEUP OF AIR BEARINGS.

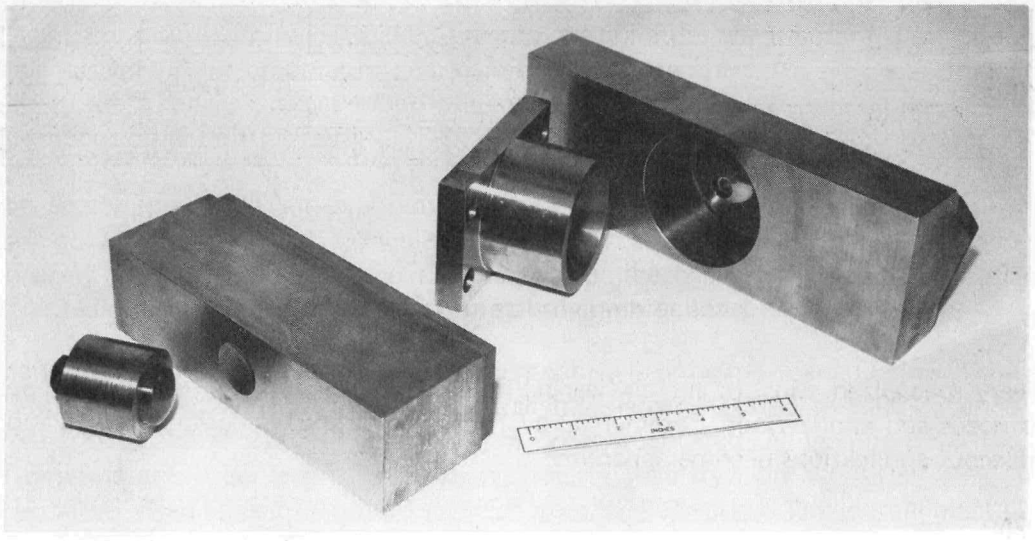

138932

Figure 7. AIR BEARING PADS WITH SELF-ALIGNING SPHERICAL SUPPORT.

In addition to the development and application of air bearings to machine-tool components tailored to fit our needs, application of commercially available components has kept pace with market availability. Unfortunately, commercial availability is still rather limited and, at the same

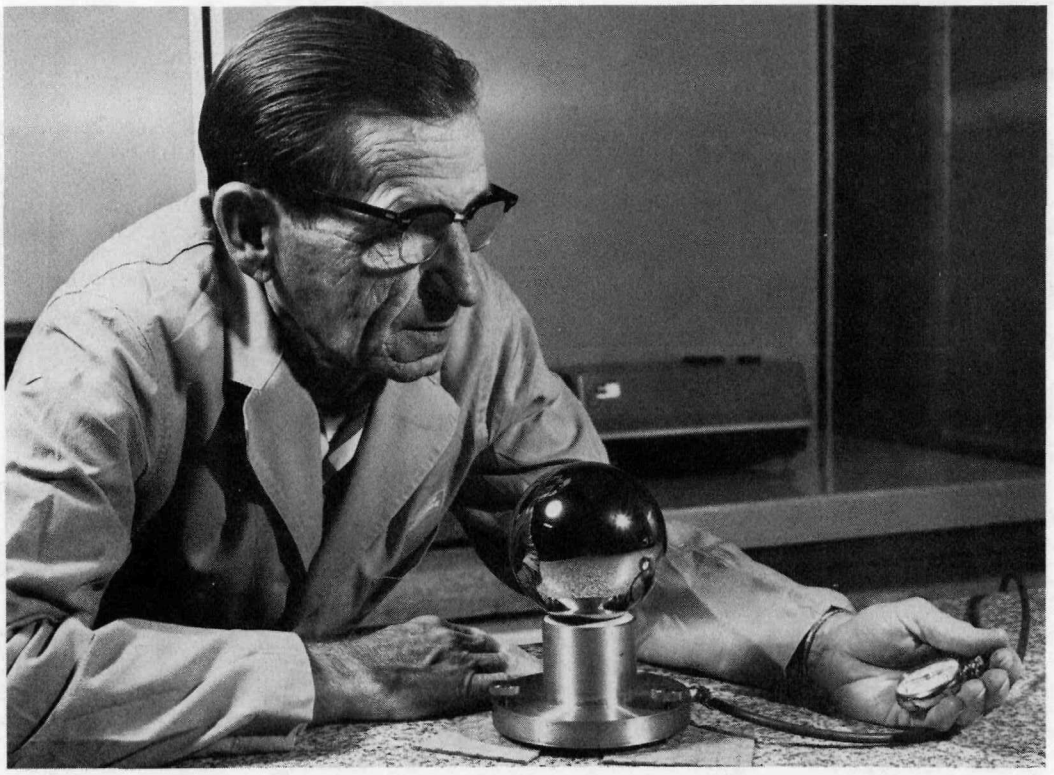

123851

Figure 8. SPHERICAL BALANCE.

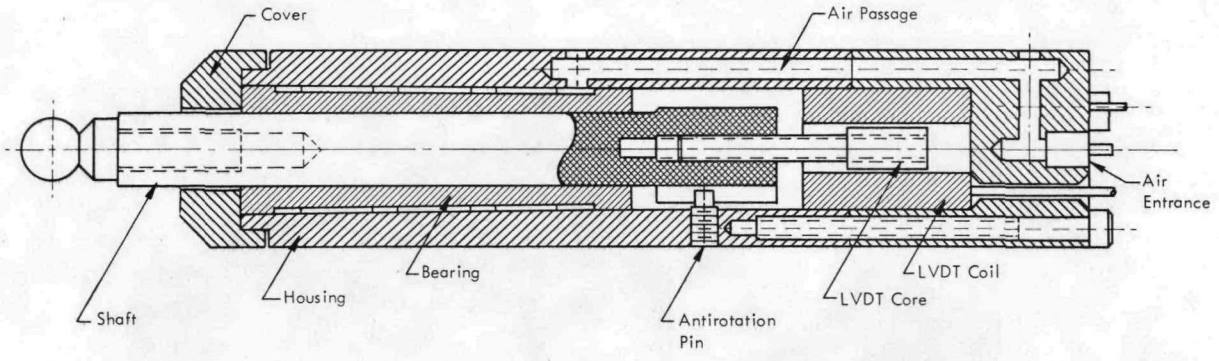

Figure 9. CROSS SECTION VIEW OF AN AIR-BEARING GAGE HEAD.

time, very specialized. Most of the air-bearing hardware purchased has been custom designed to fit our needs and applications. Commercial availability of standard components is improving as advantageous applications become apparent.

DESIGN

Practical Considerations

In most areas of technology, practical air-bearing product design and development require more than engineering analyses which evaluate performance criteria or specifications. Consideration must be given to the practical aspects of product-fabrication operation, as well as maintenance. The design of air bearings for application to the machining process is certainly no exception.

Problems associated with the fabrication of bearing geometries with 10 to 20-microinch (0.254 to 0.508 μm) tolerance on contour, and controlling the size to obtain dimensional differences of mating surfaces within a hundred microinches (2.54 μm) must be carefully considered, as must the problem of designing a component structure in which microinch alignment of bearing surfaces can be maintained when subjected to pressure forces of hundreds of pounds and part load and machining force moments of thousands of inch pounds. Bearing reliability and instability under adverse operating conditions, component assembly and installation, and repair maintenance in the event of a failure must all be considered, both from a performance and an economical vantage point.

Adjustable Self-Aligning Support

Structural distortion and close tolerance on size of mating surfaces can be eliminated or minimized through the use of adjustable self-aligning support hardware. For many applications, a fine thread will provide adequate adjustment sensitivity. In cases where microinch control is required, differential screws can be employed. Movement in this case is a function of the thread lead, the thread lead difference, and the angular rotational sensitivity.

A differential screw with one degree of angular resolution and thread leads of 1/20 and 1/22 will have a movement sensitivity of 12 microinches (0.305 μm) when properly designed. The self-alignment feature will minimize the effect of machining errors and housing distortion due to pressure forces. A typical boring or inspection ram design configuration utilizing a self-aligning adjustable support has been shown in Figure 4.

Flexured Support

Use of flexures or a low spring constant support can provide many advantages in bearing operation and performance, and can effectively reduce fabrication tolerance requirements for the critical bearing journal, thrust face, or guide rail. Flexures can be used with boring rams to minimize the effect of nonparallelism between opposite bearing surfaces, to minimize the forward movement of the face of spool-type spindles due to heat generation and resulting thermal instability, and to improve the adjustment sensitivity of bearing pads. Flexures are always used in conjunction with a nonflexured pad, resulting in something greater than half the maximum bearing film stiffness (ie, the stiffness of nonflexured captive bearings). Flexures are not generally used in a noncaptive bearing arrangement.

Stiffness of a captive bearing arrangement with a flexured pad can be determined in the same manner as the overall deflection characteristic of springs in series and parallel:

$$K = K_1 + \left(\frac{K_2 K_3}{K_2 + K_3} \right),$$

where K_1 represents the spring constant of the nonflexured air film; K_2 the spring constant of the flexured air film; and K_3, the spring constant of the flexure. The cross section of an adjustable, self-aligning, spool-type spindle, as illustrated in Figure 10, will serve to illustrate the effectiveness of flexuring the rear thrust bearing to minimize spindle growth, simplify assembly, and increase the fabrication tolerance requirements.

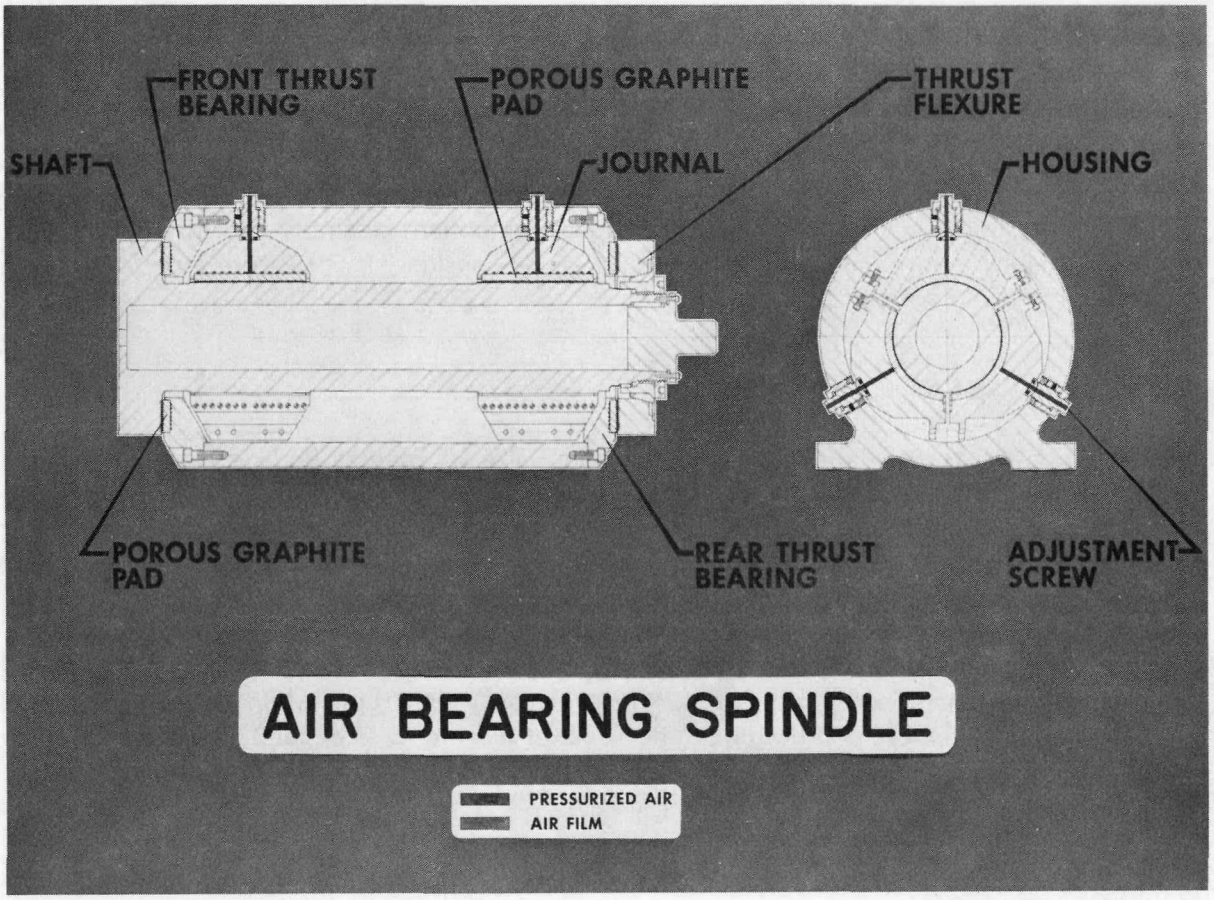

115901

Figure 10. AIR BEARING SPINDLE. (With a 3-Piece Adjustable Cylindrical Journal)

The spindle assembly is simplified in that the preloaded flexure is used to move the rear thrust forward until the film pressures reach the design level, indicating the proper film thickness. This adjustment can be made effectively for film thicknesses as low as 50 microinches (1.27 μm), providing the thrust runner accuracy and distortion under load are compatible. A high flexure ratio also permits a degree of self-alignment due to the difference in the spring constant between the flexure and rear air film. This provision reduces the fabrication tolerance requirement, especially on parallelism of the bearing thrust runners and thrust pad, and minimizes the concentricity problems between the front and rear bearings. Spindle growth can be determined from:

$$\delta = \frac{\dfrac{K_2 K_3}{K_2 + K_3}(\alpha L \Delta T)}{K_1} .$$

A two-degree fahrenheit (1.1° C) rise in the temperature of a 12-inch (304.8-mm) steel shaft with a 1-to-12 spring constant ratio will result in a forward movement of the shaft face, due to a change in the shaft length between bearings of only 12 microinches (0.305 μm).

Bearing Geometry and Arrangement

For many applications, bearing geometries can be chosen to improve the fabrication capability, component assembly, and maintenance. An example of this is the boring ram seen in Figure 4. The rectangular boring bar is readily lapped flat on a given side. By using the small, flat, adjustable, self-aligning bearing pads, the system is readily assembled; and the requirement for controlling the size and perpendicularity, both inherently and relative to the housing, is eliminated. The individual pads can be machine lapped easily to a flatness of a light band. Distortion due to pressure forces is symmetrical about the center support; and, because of the short length, is small. Maintenance to the graphite bearing is simplified by this arrangement since the pads are easily accessible without dismantling the housing.

Another example of easily fabricated geometry and arrangement is the spherical-zone bearing spindle, designed and developed for machining applications. A cross section of the spindle is indicated in Figure 1. The advantages of the spherical geometry are that the spindle bearings are self-aligning, and the journal can be lapped with conventional equipment to microinch accuracy by using chordal lapping techniques. Here, as with the spool-type spindle, supporting the rear journal on an adjustable flexured support minimizes fabrication errors and tolerance requirements, and allows quick assembly and disassembly.

DESIGN PROCEDURES

In designing the externally pressurized air-bearing components for machine-tool application, two considerations were of greatest importance: load capacity and compliance. For spindles, heat generation in the bearing film and its influence on thermal stability of the component was also considered important. From past experience it was found that reasonably accurate results for predicting the deflection of a member due to side loading could be obtained using resultant forces and treating the movement member as a free beam. The forces, considered to be acting on the spindle system, as illustrated in Figure 11. Total deflections of the spindle are a combination of beam bending and bearing and structure deflection. In most cases the structure is considered rigid and neglected.

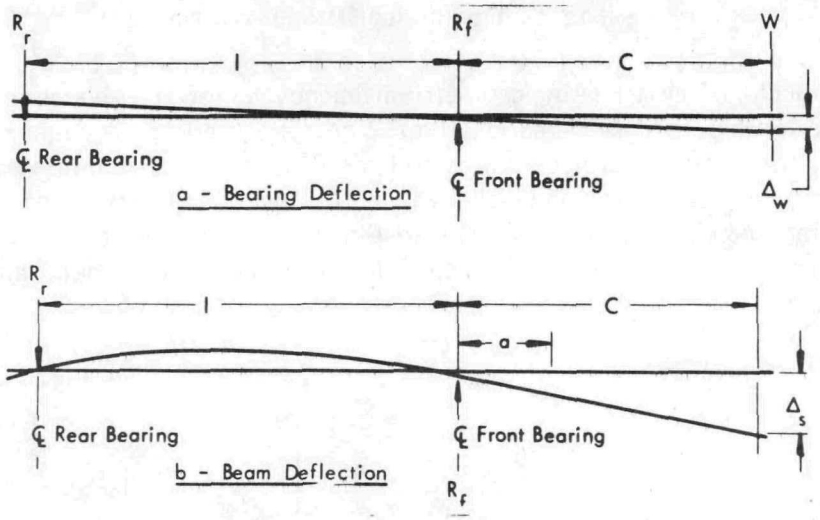

Figure 11. FREE BODY DIAGRAMS FOR DETERMINING SPINDLE SHAFT DEFLECTION.

When calculating film deflection, two projected areas are used. Normally, only the area opposed to the load would be used; but, since the area in line with the load will have a decreasing pressure acting on it as a result of film deflection, it also is used. With reference to the loading diagram shown in Figure 11, the deflections were calculated from:

$$\Delta_W = \frac{l+c}{l}\left(\frac{R_f}{2As}\right)+\frac{c}{l}\left(\frac{R_r}{2AS}\right).$$

Static-bearing film stiffness was determined experimentally for a captive system and can be approximated by $S = E_f\ 0.35\ P_s/h$ over the operating range, for a captive bearing system, where the film thickness on both sides of the bearing journal or runner is equal, and the average film pressure for the initial or unloaded condition is approximately 55% of the supply pressure. Typical pressure distribution for a flat pad is shown by the graph of Figure 12. Pressure profile, film stiffness, and bearing flow were measured for a 4 by 4-inch (101.6 by 101.6-mm) test-pad arrangement equipped with static pressure taps, strain-gage instrumented support structure, and a precision flow meter. An estimate of average pressure for a different initial film thickness can be made from these curves.

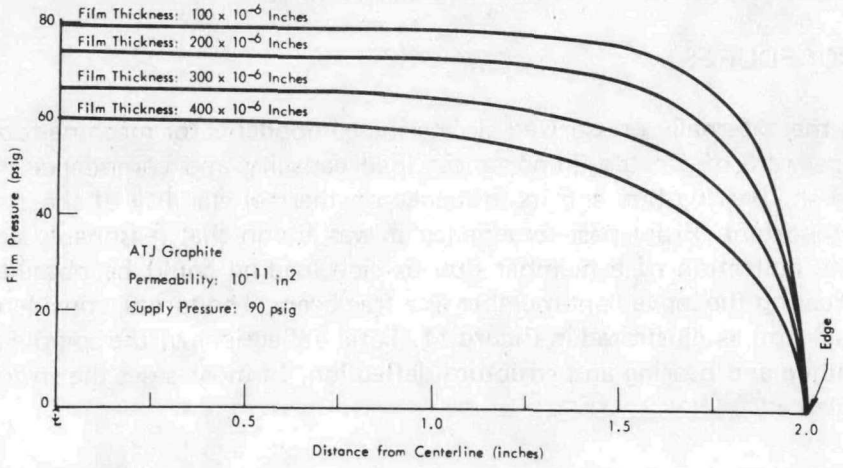

Figure 12. TEST BEARING FILM PRESSURE PROFILES

E_f can be thought of as a bearing-geometry efficiency factor and relates the flat-film-stiffness empirical relationship to curved-bearing films. For a flat pad, E_f is equal to one. Expressions were derived, based on the projected area and the film-thickness variation as a function of the projected area, for cylindrical and spherical-bearing geometry. The need for this expression results from relating flat-film data to a curved film because of the nonlinear relationship which exists between centerline deflection (eccentricity for a cylindrical shaft) and the bearing film thickness change.

For cylindrical geometry:

$$E_f = \frac{\frac{\theta}{2}+\frac{\sin 2\theta}{4}}{\sin\theta}\Bigg]_{\theta_1}^{\theta_2}.$$

For spherical-zone geometry, deflection due to forces normal to the shaft centerline (see Figure 3):

$$E_f = \frac{\left(\sin\beta - \frac{\sin^3\beta}{3}\right)\Big]_{\beta_1}^{\beta_2} \left(\frac{\theta}{2} + \frac{\sin 2\beta}{4}\right)\Big]_{\theta_1}^{\theta_2}}{\left(\frac{\beta}{2} + \frac{\sin 2\beta}{4}\right)(\sin\theta)\Big]_{\theta_1}^{\theta_2}} .$$

Theta (θ) lies in the planes normal to the spindle centerline and is zero along the plane in which the resultant force vector lies. Beta (β) lies in the planes normal to the planes of theta which pass through the bearing geometry centerline and is zero along the plane normal to the bearing centerline which passes through the bearing spherical center.

Beam or shaft deflection due to bending is calculated using the following equations:

$$y_a \text{ (deflection at } \underline{a}) = \frac{Wa}{2EI}\left(ca - \frac{a^2}{3} + \frac{2cl}{3}\right),$$

$$\left(\frac{dy}{dx}\right)_a \text{ (slope of beam at } \underline{a}) = \frac{W}{EI}\left(ca - \frac{a^2}{2} + \frac{cl}{3}\right), \text{ and}$$

$$\Delta_S = y + (c - a)\frac{dy}{dx} .$$

The total deflection is:

$$\Delta_t = \Delta_W + \Delta_S .$$

Axial deflection can be determined by resolving the axial forces to centered axial forces and moments. The moment serves to change the side-deflection characteristics; and, if significant, must be evaluated using the previously discussed equations. Axial deflection due to a concentric force is calculated from:

$$\Delta_a = \frac{F}{A(S)} .$$

Load capacity of the bearing can be estimated from the film-deflection equations by allowing delta (Δ) to increase to a value considered appropriate for the application. That is, for spindles operating at moderate to high surface speeds, 50% of the total film might be considered suitable; for slides or spindles operating at a low surface speed, 80% might be considered satisfactory.

Heat is generated in a hydrostatic bearing due to a shearing friction in the film as the shaft rotates. Since thermal stability is usually one of the prerequisites of an air bearing spindle, it is necessary to consider this factor in its design. The heat generated in the film can be predicted from:

$$q = \frac{2\pi MN}{720J},$$

where:

$$M = \frac{\mu r A_s V}{h} .$$

For the case of a spherical zone bearing:

$$M = \frac{0.66\ N\ \mu r^4}{h} \int_{\theta_1}^{\theta 2} \sin^4 \theta\ d\theta\ ,$$

where:

Q represents the heat generated in the bearing (Btu/s),

M the friction moment (inch lbs),

A the surface area of the bearing (in^2),

h the film thickness (in),

N the shaft speed (rpm),

J the conversion constant (778 ft lbs/Btu), and

r the spherical radius of the bearing (in).

The volumetric air flow rate through the bearings was predicted from an equation derived from Euler's equation for steady, one-dimensional flow with friction, neglecting the body force of weight and inertia for compressible fluid flow through a slot and modified for use with porous material. The derived equation used to predict air flow from a recessed bearing is:

$$Q_2 = \frac{bh^3}{24\mu l_s P_2} \left(P_1^2 - P_2^2 \right) .$$

Measurement of pressure profiles for porous bearings where the air film is fed over the entire area indicates a relatively flat profile very similar to that of a recessed bearing. This same equation can be used to effectively predict bearing flow by modifying the equation with an effective slot length term. An expression for l_s was derived from pressure profile data obtained from the same test-bearing arrangement used to determine film stiffness, namely:

$$l_s = 1.6 \times 10^3 P_f^{0.6} h^{1.4} .$$

Several different grades of graphite were investigated for air-bearing application. Darcy's equation was used to calculate the permeability of the material. This equation is:

$$Q_2 = \frac{KA \left(P_1^{\ 2} - P_2^{\ 2} \right)}{2\mu T P_2} .$$

All were found to vary considerably in regard to permeability and surface porosity. As a result, it was necessary to provide a means for obtaining the restriction necessary for optimum bearing performance. In initial designs, standard pressure-compensating devices were used, such as orifices and flow control valves; but, both had the disadvantage of being located physically far enough away from the film to provide a plenum for air between the film and restrictor, primarily the storage capacity of the porous graphite.

These same initial bearing applications indicated that there was sufficient restriction in the graphite so that adequate damping was present for stable operation. Several spindles were fabricated, bench tested, and installed on production turning and boring machine tools. Unfortunately, under an operating condition of a large mass moment, as would occur with long parts and fixtures of significant weight, a self-excited instability occurred with several of the spindles. After considerable investigation by engineers at both Y-12 and the Franklin Institute Research Laboratories,(b) it was determined that the prime cause of instability resulted from excessive available porosity in the graphite at the bearing/film surface. As a result, a method of surface impregnation was developed for the graphite which increased the restriction to film backflow and effectively reduced the available porosity by an order of magnitude. At the same time, the flow characteristics of the material were modified to establish both uniformity and the desired permeability. This development was a very significant breakthrough, for it also established a model for design which is simpler to analyze mathematically. This improvement has resulted in better design guidance, especially for analyzing bearing stability.

With this technique, adjustable restrictors can still be used to optimize a system based on design deviations due to fabrication tolerances. With impregnation, self-excited instabilities are no longer a problem with captive systems and can generally be eliminated through proper design in noncaptive systems. The method presently being used is reversible so that an over application or error in calculations can be corrected without fabrication requirements. Also, as the material is applied to the finished bearing surface, it can be measured immediately, changed at will, and cover a small enough area to establish surface uniformity. Several materials have been used; but, at present, an acrylic lacquer is preferable. The techniques of this process will be covered in the section that follows. Complete sample design calculations for a 6-inch (152.4-mm)-radius spherical-zone spindle is included in the Appendix.

FABRICATION

In general, each porous graphite air bearing, regardless of configuration, consists of a graphite bearing material glued to a metal support structure. Preparation of the graphite involves gluing to the metal support and lapping to fit the metal journal or runner. After final lapping, the graphite is impregnated to obtain the desired flow restriction.

A likely chronological order of fabrication steps would be: (1) machine all components; (2) glue the graphite liner to the metal support; (3) lap, grind, or machine the metal journals or runners to the desired geometry; (4) lap graphite bearing to obtain the desired clearance with the metal journal or runner; (5) impregnate the graphite to obtain the proper air flow; (6) assemble.

Fabrication steps and features peculiar to the graphite air bearing, specifically to the spherical-zone spindle, will now be explored in detail. It will become obvious that much of the following information is applicable to any geometry.

(b) Franklin Institute Research Laboratories (FIRL), Philadelphia, Pennsylvania.

Construction details of the bearings, housing, and rotating element are shown in Figures 13, 14, and 15, respectively. None of the machining tolerances are critical except for the spherical journals and the bearing surface of the carbon. In order to obtain the desired geometry accuracy of the spherical-zone bearing journals, they were machined on a precision 15 by 15-inch (381 by 381-mm) tape lathe which had been modified with the first fabricated air-bearing spindle. The results obtained were quite satisfactory. Inspection results of the 6-inch (152.4-mm) spherical radius, hardened stainless steel (RC 50) bearing journals after machining indicated an average roundness of 20 microinches (0.508 μm) TIR, a sphericity of $\pm$ 200 microinches ($\pm$ 5.08 μm), and a spherical radius of 6.000 $\pm$ 0.0003 inches (152.4 $\pm$ 0.00762 mm). Surface finish varied from 10 to 30 microinches (0.254 to 0.762 μm), rms.

An alternate method is to chordal lap the metal journals to the desired geometry. This is a method used to lap spherical surfaces to less than a 20-microinch (0.508-μm) deviation from true sphericity with relative ease. The basic setup is depicted in Figure 16. The journal is placed on a rotating table, then a lap is placed on the journal. The lap must be free to move in a nearly radial direction and to rotate. One means of obtaining such freedom is to mount the lap on a ball seat on a shaft that is free to slide in a sleeve bearing. Thus, the only force between the lap and journal is the weight of the lap. The part is driven and, in turn, drives the lap. For self cleaning, at least ten equally spaced grooves should be cut in the lap which is preferably made of cast iron. To obtain the minimum lapping time, the lap should make line contact with the journal. Figure 17 provides a comparison between a good lapping surface and a poor one. Periodic remachining of the lap is recommended in order to assure a good surface.

Lapping compound having particles from 5 to 10 micrometres in diameter is generally suitable. Diamond and silicone carbide particles are preferable, but aluminum oxide has been used successfully. Oil should be used as a lapping vehicle, but care should be taken to avoid excess oil as the lap will merely glide over the oil film and do very little cutting. Rotational speed of the journal should be varied for best results (10 to 20 rpm is a normal speed range). Generally, too high a speed causes flotation of the lap and slow material removal. Too low a speed, on the other hand, causes stick slip, vibration, and erratic material removal.

Gluing of the graphite liner to the metal support housing is an extremely important step. A faulty bond can lead to bearing failure at a later date. A metal-loaded epoxy resin is recommended. The metal particles in the resin

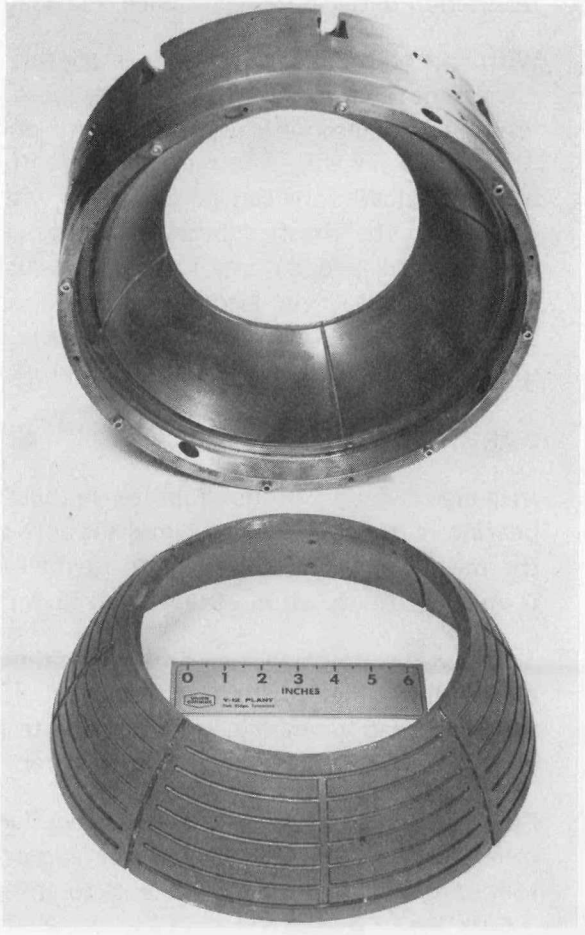

121032

Figure 13. CARBON LINER AND AIR-DISTRIBUTION GROOVES OF A BEARING HOUSING.

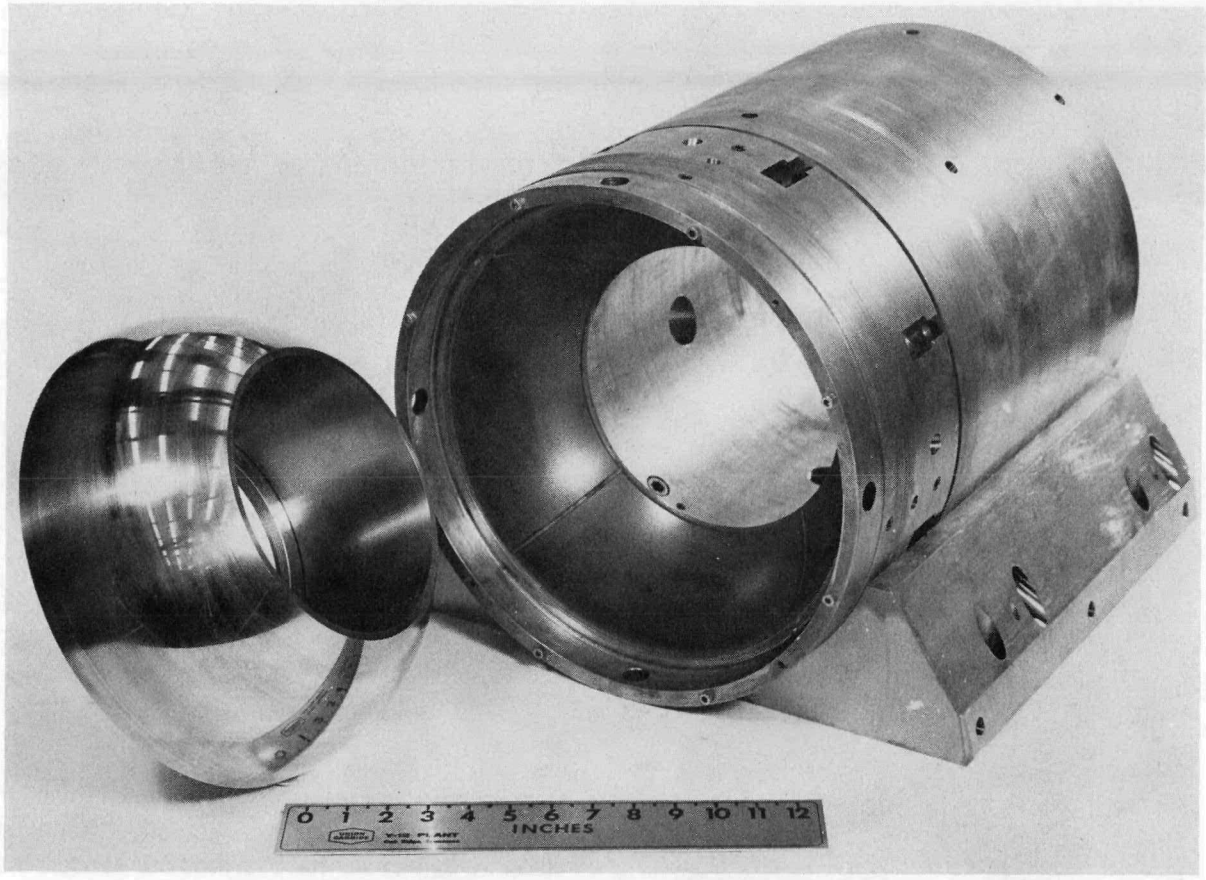

121033

Figure 14. SPINDLE HOUSING AND MOUNTING PAD.

help prevent the resin from being soaked up into the graphite. Manufacturer's directions should be followed as to surface preparation, cure time, and temperature. An even coat of resin should be applied to the graphite surfaces which will contact the metal. Some type of weight is advisable for maintaining contact during cure.

After the epoxy has cured, all exposed surfaces of the graphite that are not bearing contact surfaces should be coated with a clear epoxy, taking care not to allow any to collect on the actual bearing surfaces. When the coating has cured, the bearing should be pressurized with 60-psig (413-kPa) air for a day to verify the metal-to-graphite bond.

After the journal has been chordal lapped, the graphite bearing may be lapped with the journal. It is advantageous to have the journal radius slightly larger [0.0005 to 0.001 inch (0.012 to 0.025 mm)] than the graphite liner material in order to shorten the lapping time (Figure 17). Figure 18 shows the basic setup. The bearing housing is placed on a rotating table, then the journal is placed at an angle of from 10 to 45 degrees to the bearing. The journal must be free to rotate and to move axially. Rotating the housing at a speed of between 5 to 15 rpm provides good results. Aluminum oxide lapping compound should be used, which approximates the film thickness [ie, a 5-micrometre compound yields an approximate 200-microinch film (5.08-μm)]. The compound should be mixed with ethyl alcohol or water in a ratio by volume of approximately ten parts of alcohol or water to one of the compound. A bottle of water or alcohol should also be on hand with which to wet and clean the bearing while lapping. Precautions should be taken to prevent a buildup of loose graphite. Lapping is completed when

121031

Figure 15. SPINDLE ROTATING ELEMENT.

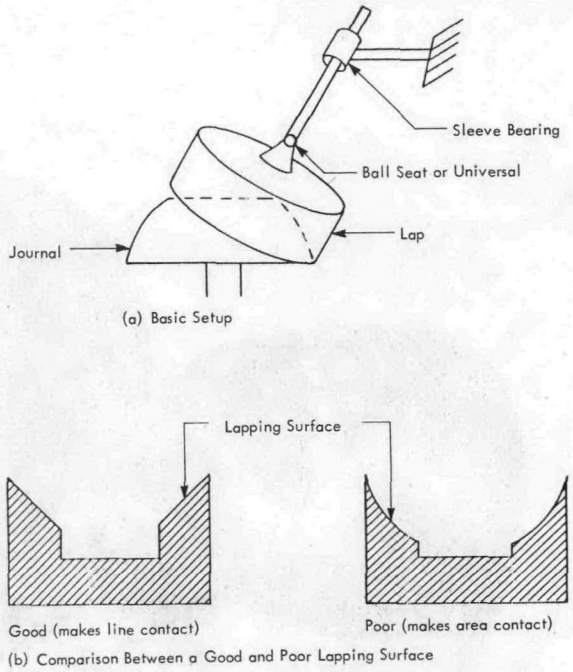

Figure 16. CHORDAL LAPPING.

the newly lapped finish is present over the entire bearing surface. After all surfaces are lapped, the graphite bearings are ready to be impregnated.

Impregnation of porous graphite is a procedure which changes the effective permeability of the graphite to obtain the proper flow to the bearing and to improve the bearing's resistance to self-excited instability or "pneumatic hammer".

Essential to the impregnation technique is the apparatus with which to measure the

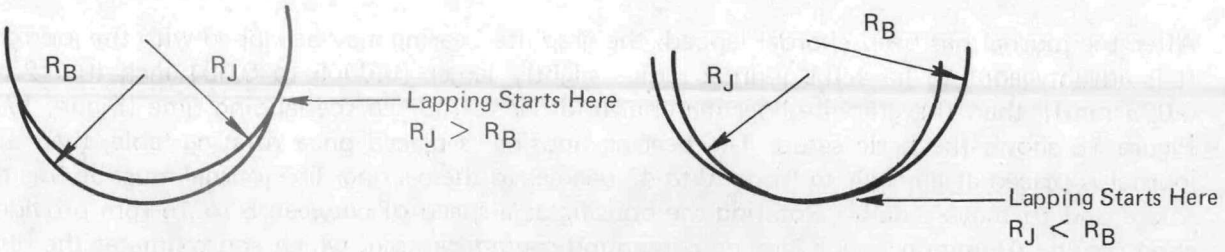

Figure 17. ZONAL LAPPING POSITIONS.

permeability (Figure 19). This apparatus consists of a stethoscope-type probe connected to a flowmeter. When the probe is pressed against the graphite, the flow can be measured through an

area of the graphite equal to that covered by the probe. Darcy's equation can then be used to calculate the permeability:

$$Q_2 = \frac{KA\left(P_1^2 - P_2^2\right)}{2\mu T P_2},$$

where:

Q_2 represents the volumetric rate of flow measured at Point P_2,

K the permeability,

A the area,

μ the viscosity, and

T the thickness between Points 1 and 2.

The advantages of this method are: (1) permeability can be measured on actual bearings without causing damage, (2) the method is quick and fairly accurate, and (3) the apparatus is inexpensive and portable.

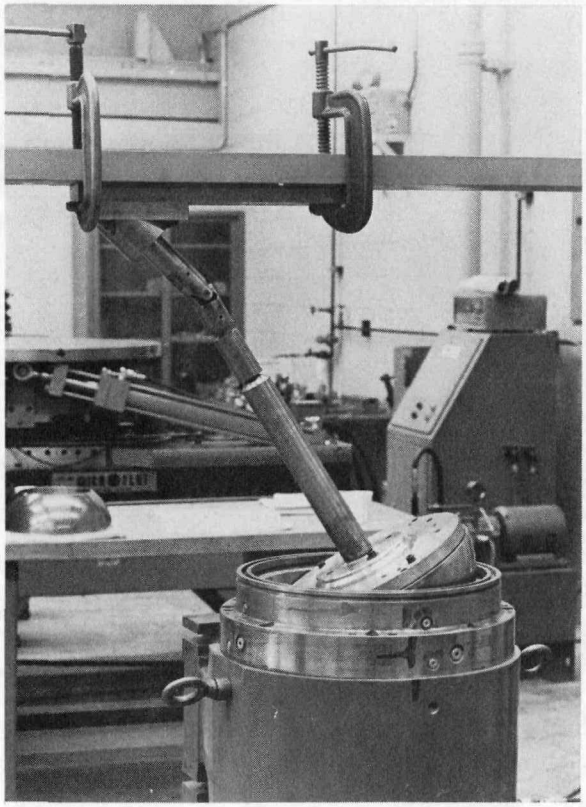

145492

Figure 18. ZONAL LAPPING SETUP.

Acrylic lacquer dissolved in methylene chloride is the impregnating substance. Features of this material which make it advantageous are: (1) it has a softening temperature higher than temperatures ordinarily experienced in routine operation, (2) it has good bondability to the graphite, (3) it has good permeability, and (4) it possesses ease of preparation and application.

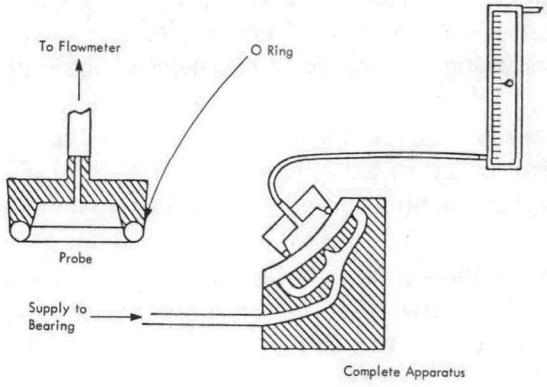

Figure 19. PERMEABILITY MEASURING APPARATUS.

The procedure for impregnation is as follows:

1. Mix the impregnating solution in the ratio of one part acrylic lacquer to three parts methylene chloride by volume. Cover the solution when not in use to reduce evaporation of the solvent from the mixture.

2. Turn the bearing supply pressure to 40 psig (276 kPa) and measure the flow rate and uniformity over the bearing surface (see Figure 20).

3. Change from a 40-psig supply pressure to a 25-inch (hg) (84.5-kPa) vacuum at the bearing.

4. Wet a small area of tissue, cotton pad, or soft clean cloth with impregnating solution and rub the liquid onto the bearing surface (Figure 21).

5. Reduce vacuum to ambient conditions. Wipe the bearing surface with a clean tissue, cotton pad, or cloth dampened with methylene chloride (Figure 22).

6. Allow approximately one minute to dry. (Time can be shortened by using a heat blower.)

7. Turn the bearing supply pressure to 40 psig (276 kPa) and measure the flow with a probe. Reading should be lower than required. If not, repeat Steps 3 through 6 (Figure 23).

8. Establish a pressure of 5 psig (34.5 kPa) at the bearing and wipe the graphite surface with cloth, tissue, or pad dampened with methylene chloride (Figure 24).

9. Allow sufficient time for the surface to dry.

10. Turn the bearing supply pressure to 40 psig (276 kPa) and measure the flow with the probe (Figure 25).

11. Repeat Steps 8 through 10 until the bearing flow is within an acceptable tolerance.

12. If the flow measurement made in Step 11 exceeds that desired, return to Step 5 and proceed.

Impregnation should be done under an exhaust hood or in a well-ventilated area. Precautions should be taken to avoid skin irritations which can result from contact with the solvent (methylene chloride). Regular cleaning solvents should not be used on the impregnated surface. If cleaning is required, a chemical which will not affect the impregnated lacquer should be used.

When properly applied, the lacquer is deposited in a layer that penetrates from the surface to a depth of 20 to 50 mils (0.5 to 1.25 mm). Figure 26, Views (a) and (b), shows scanning electron microscope photographs of impregnated and unimpregnated graphite.

Most importantly, impregnation can improve a bearing's dynamic stability. Figure 27 provides data that were obtained on a test bearing before and after impregnation. The region to the right of the curve is unstable.

Impregnation also has alleviated an instability in a 6-inch (152.4-mm)-radius spherical air-bearing spindle. Before impregnation, the spindle would hammer at a load of over 150 pounds (667 N),

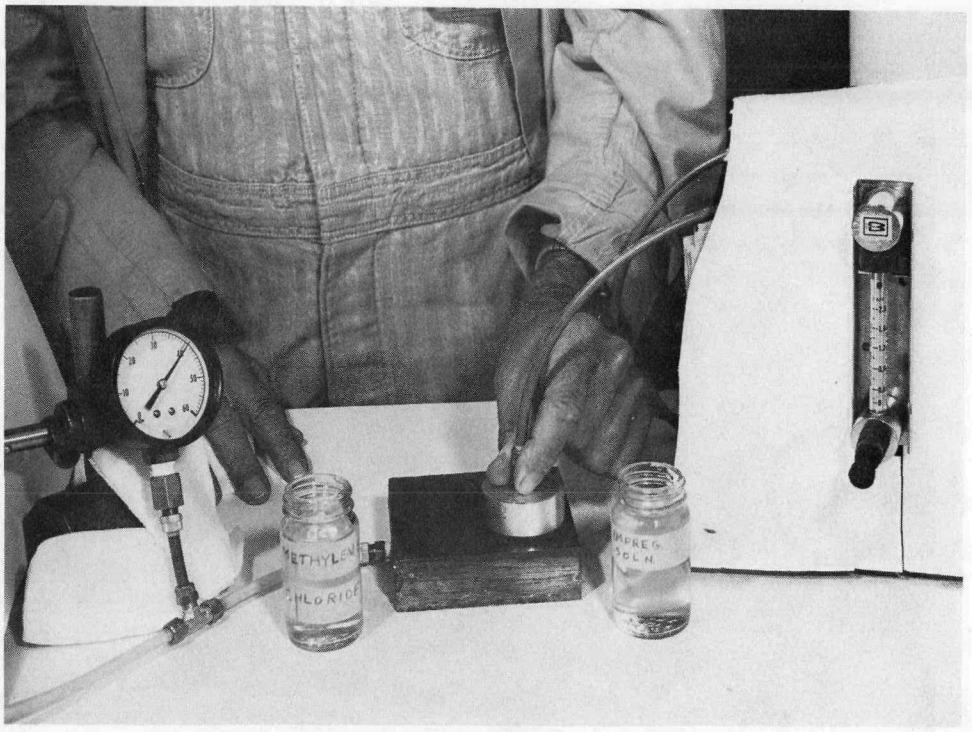

147118

Figure 20. CHECKING INITIAL FLOW CONDITION.

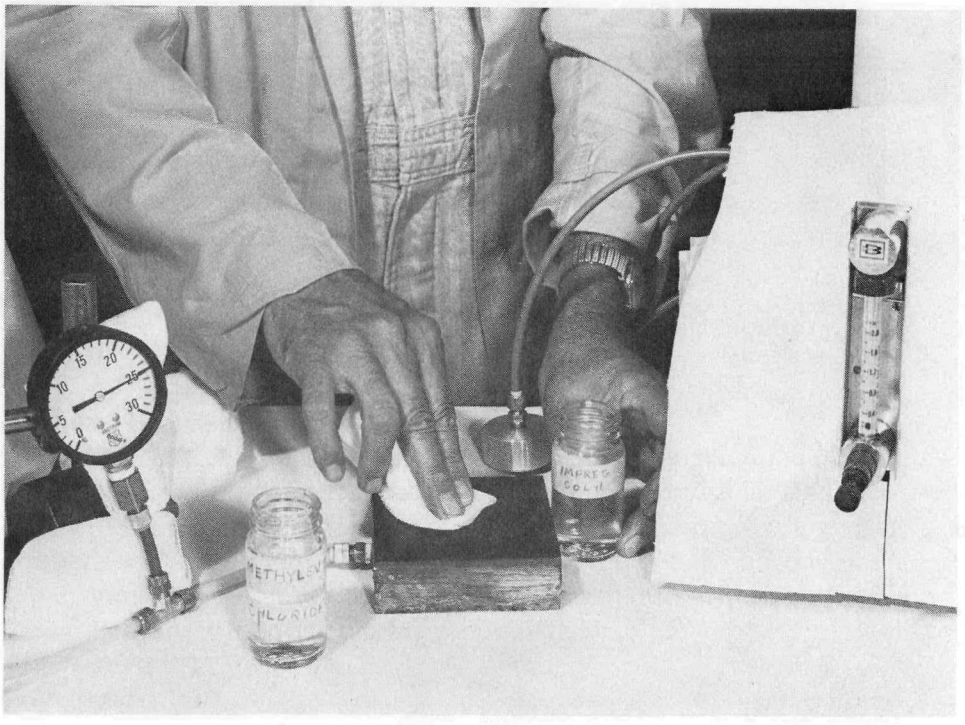

147116

Figure 21. IMPREGNATION PROCEDURE. (Rubbing Liquid Onto Bearing Surface)

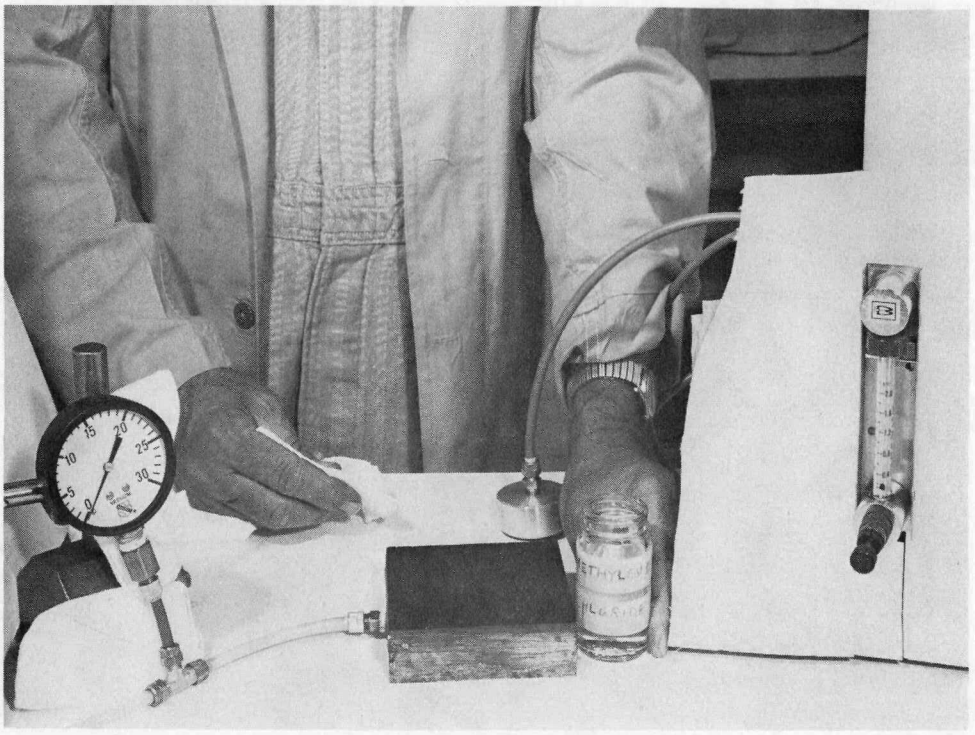

147115

Figure 22. IMPREGNATION PROCEDURE. (Wiping the Bearing Surface)

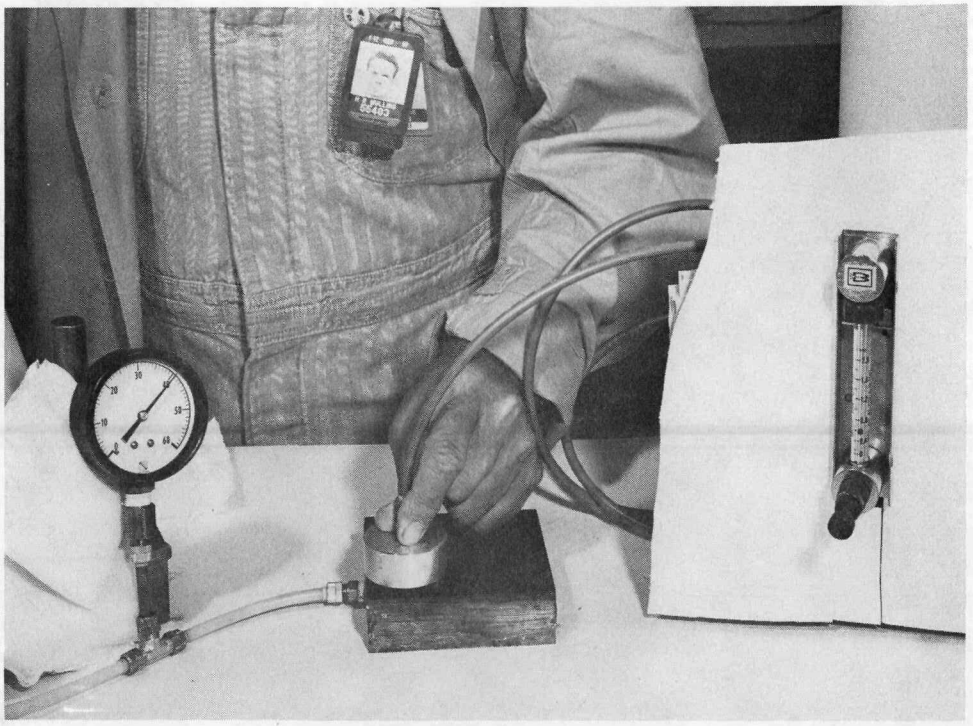

147117

Figure 23. IMPREGNATION PROCEDURE. (Second Measure of the Flow Rate)

147119

Figure 24. IMPREGNATION PROCEDURE. (Rewiping the Bearing Surface)

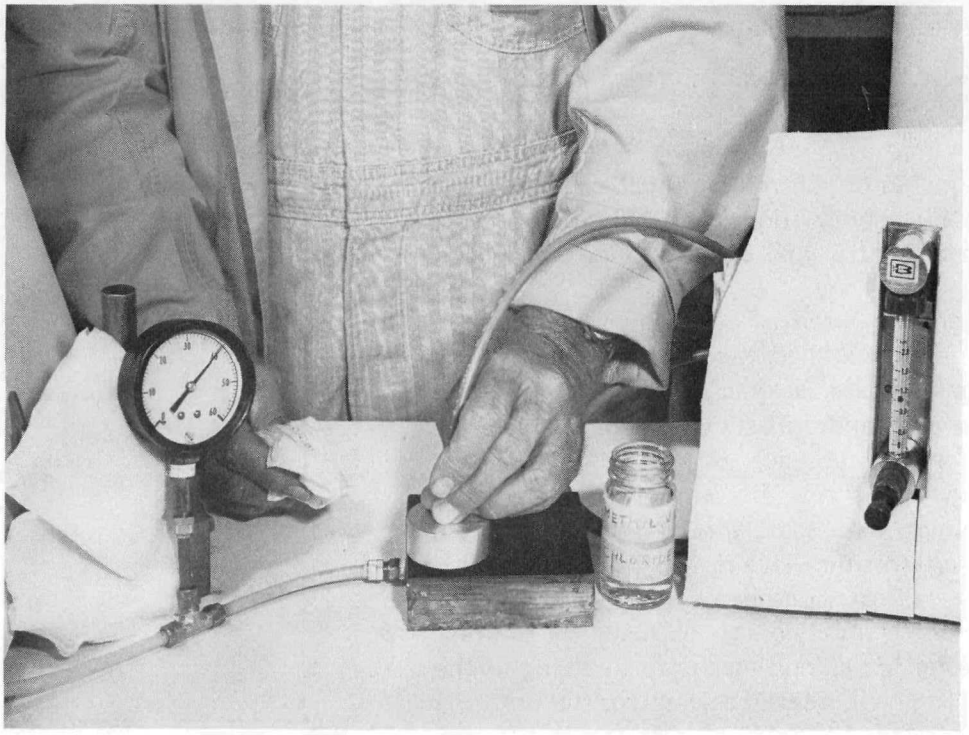

147120

Figure 25. IMPREGNATION PROCEDURE. (Final Measure of Air Flow)

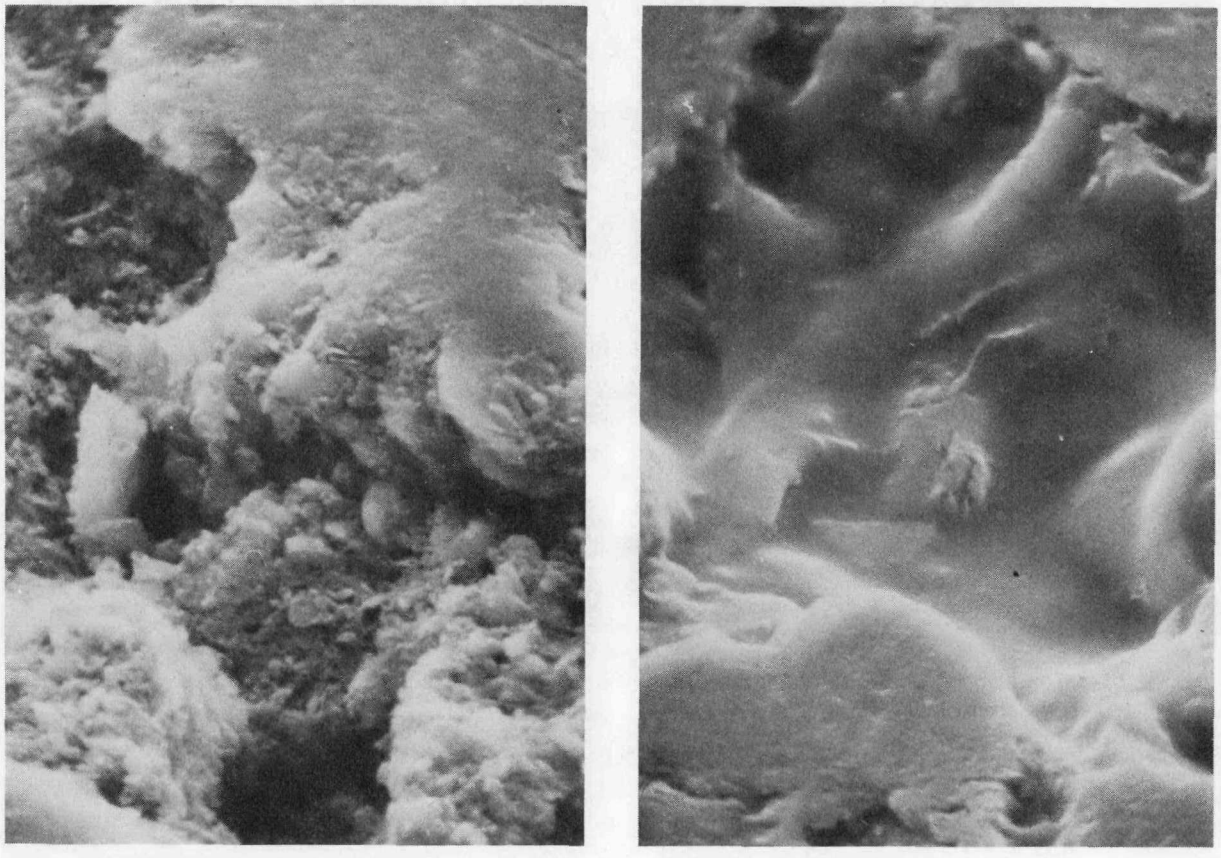

(a) Unimpregnated Graphite

(b) Impregnated Graphite

Figure 26. SCANNING ELECTRON MICROSCOPE PHOTOGRAPHS OF UNIMPREGNATED AND IMPREGNATED GRAPHITE. (1000X)

12 inches (304.8 mm) from the spindle face. After impregnation, no vibrations were observed at a load of 500 pounds (2224 N).

After the bearing components have been lapped in matched pairs and impregnated, the front segment is attached to the shaft using face bolts and a plastic compound which sets up in the absence of air to produce an equivalent shrink fit between the shaft and segment. The shaft should be next set in a vertical position face down. The housing, also in a vertical position, is gently lowered upon the shaft until contact is made at the rear bearing. After bolting the flexure ring to the rear segment, the subassembly is slid onto the shaft until the segment is seated in the rear bearing pad. The flexure ring is preloaded by a nut threaded onto the shaft. The spindle assembly is then set in a horizontal position and bolted to a test surface or slide.

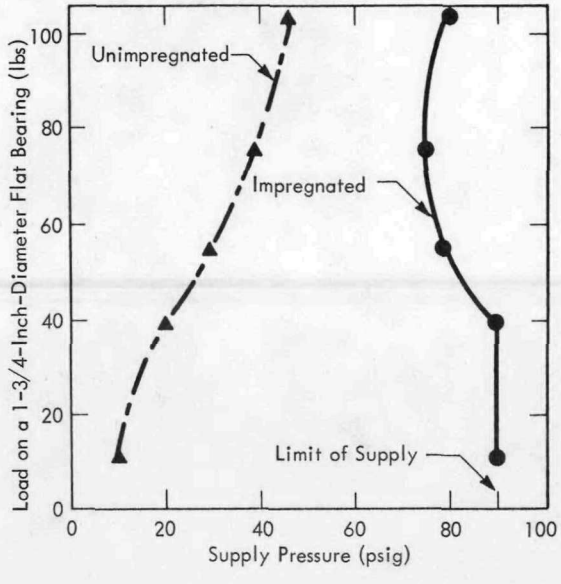

Figure 27. STABILITY OF IMPREGNATED VERSUS UNIMPREGNATED AIR BEARING.

After connecting the air-supply tubing and pressurizing the bearings, the rear bearing and flexure assembly are tightened until the axial movement that takes place in pressurizing the bearings is approximately 450 microinches (11.43 μm). This value gave a film clearance of approximately 300 microinches (7.62 μm), the desired operating clearance.

PERFORMANCE EVALUATION

Performance characteristics should be measured for each spindle. The characteristics and test procedure, as described, relate directly to the previous testing of a six-inch-radius spherical-zone spindle; however, any size spindle could be tested in the described manner by modifying the procedure to suit the geometry of the spindle. The tests to be performed are:

1. Static radial deflection as a function of load at the spindle face and at a point 6 inches (152.4 mm) in front of the spindle.

2. Static axial deflection as a function of load at the spindle center of rotation.

3. Radial motion, both at a point 2 and 8 inches (50.8 and 203.2 mm) in front of the spindle face.

4. Axial motion.

5. Spindle growth at 1000 and 2000 rpm (forward movement of the face measured relative to the spindle mounting surface).

6. Temperature increase of the bearing housing's spindle face and the surface of the mounting plate at a point forward and to the side of the spindle. (One of the spindles being tested is shown in Figure 28.)

Spindle growth and deflection characteristics are presented graphically in Figures 29 and 30. The equipment arrangement used to measure the deflection rates is shown in Figure 31. Applied force was measured with a force gage; deflection was measured with a noncontact gage. For radial deflection, a precision standard was mounted on the spindle face and aligned within 30 or 40 microinches (0.75 or 1.0 μm). The proximity transducer, located near the surface of the standard, was used to measure the horizontal movement of the spindle centerline. With this arrangement, the effects of a slight mount of spindle rotation due to the applied load do not show up in the deflection measurements. For the case of radial deflection at the face, the load was applied at the face while deflection was actually measured 2 inches (50.8 mm) in front of the face, the approximate length of the standard. For the case of radial deflection 6 inches (152.4 mm) from the face, the load was applied to an 8-inch (203.2-mm)-diameter cylinder bolted to the spindle face and the deflection was measured at a point 2 inches (50.8 mm) in front of the point of load application, a total of 8 inches (203.2 mm) in front of the face. All measurements were made relative to the spindle mounting plate and therefore included housing deflections as well as bearing and shaft deflections. This method provides a measure of the deflection that will occur due to the spindle during production use.

Spindle growth was measured using a noncontact gage located near the spindle face for continuous speeds of 1000 and 2000 rpm. Temperature of the bearings was measured at the outer surface of the housing about midpoint of the bearing length. Spindle-face temperature was measured upon stopping the spindle shaft after apparent steady-state conditions were reached.

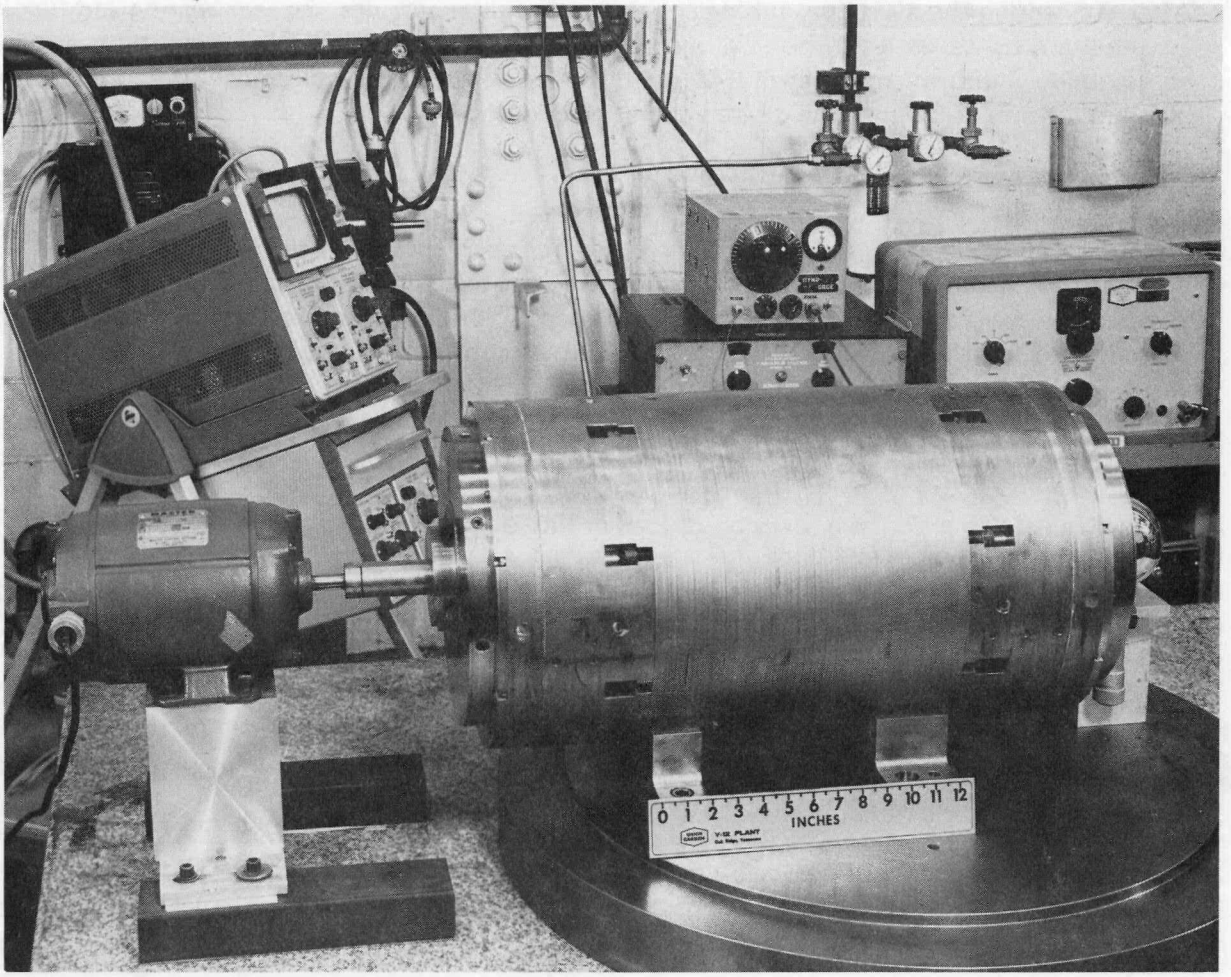

121030

Figure 28. AIR-BEARING SPINDLE BEING TESTED.

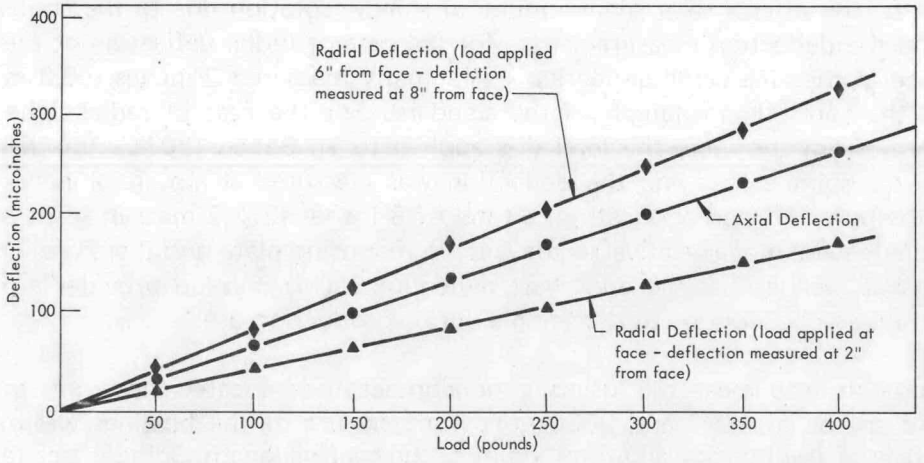

Figure 29. SPINDLE DEFLECTION. (Spindle 3)

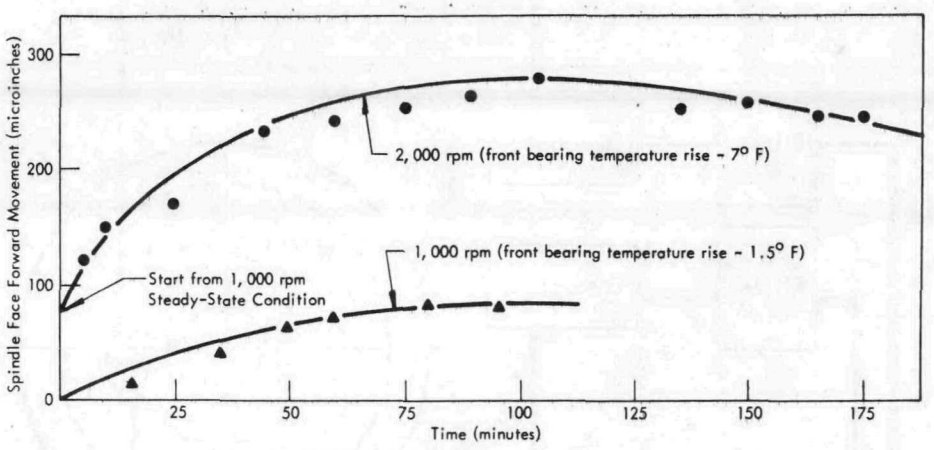

Figure 30. SPINDLE GROWTH. (Spindle 3)

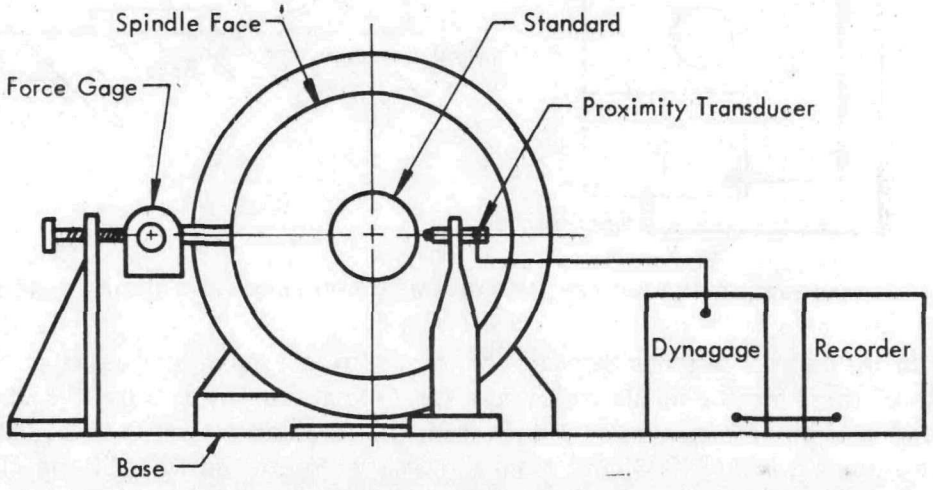

Figure 31. TEST EQUIPMENT FOR MEASURING DEFLECTION.

Temperature rise and spindle growth varied in a similar manner with time; only the maximum temperature reached is shown in the figures. Maximum spindle-face temperature and front-housing temperature were approximately the same.

Radial motion of the spindle axis of motion was made using a hemispherical standard (accurate within 2 μin) mounted 20 to 30 microinches (0.508 to 0.762 μm) off center on the spindle and two noncontact gages. The proximity transducers were set at right angles with each other with outputs displayed after filtering at different levels with the filters, in the form of a lissajous pattern on a storage oscilloscope. With this method, and for a perfect standard, zero motion of the spindle centerline would be displayed as a true circle on the oscilloscope, with radius being a measure of the misalignment of the center of revolution of the standard and the spindle center of rotation. Deviation from a true circle is a measure of the combination of the standard and spindle errors, and the inaccuracies of the measuring system. The measuring system, when properly calibrated, has a probable accuracy that is ± 10% of the range of measurement. The system arrangement is presented in Figure 32.

A typical lissajous pattern is shown in Figure 33. Axial motion was measured using the same standard with a single noncontact gage. The proximity transducer was located at the pole of the standard and the movement displayed in a wave form on the oscilloscope. Axial motion was

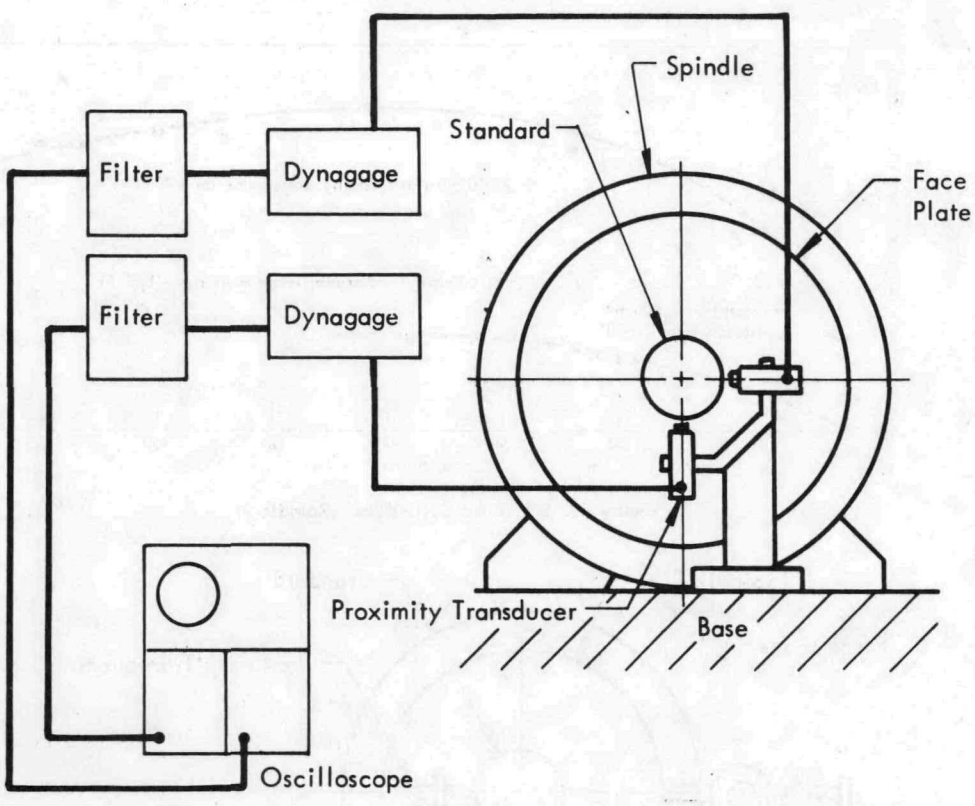

Figure 32. TEST EQUIPMENT ARRANGEMENT FOR MEASURING RADIAL RUNOUT.

equal to the vertical distance between the minimum and maximum peaks of the wave pattern. Results of these measurements indicated a total radial motion of 6 to 10 microinches (0.15 to 0.25 μm) at a point 2 inches (50.8 mm) from the face and 10 to 12 microinches (0.25 to 0.30 μm) at a point 8 inches (203 mm) from the face for speeds up to 1500 rpm. Roundness of the standard used for these measurements was 3 microinches (76.2 nm). Axial motion measured varied from 6 to 10 microinches (0.15 to 0.25 μm) for the same speed range.

In addition to these tests, measurements were made to determine the dynamic behavior of the air-bearing spindle under the influence of varying conditions of applied force. The data obtained were used to derive an equation of motion which describes this behavior. Measurements were made in the horizontal plane, using a high-speed noncontact gage and a memory-type oscilloscope equipped with a camera to record spindle deflection as an impulse force was applied to the spindle. This recorded deflection, as shown in Figure 34, is typical of the solution of a second-order linear differential equation. The derived equation of motion is an equation of this type which fits the measured data.

The general form of the equation is:

$$A_2 \frac{d^2y}{dt^2} + A_1 \frac{dy}{dt} + A_0 y = F\,\delta(t),$$

where:

F	represents the magnitude of the applied force,
$\delta(t)$	the impulse function, and

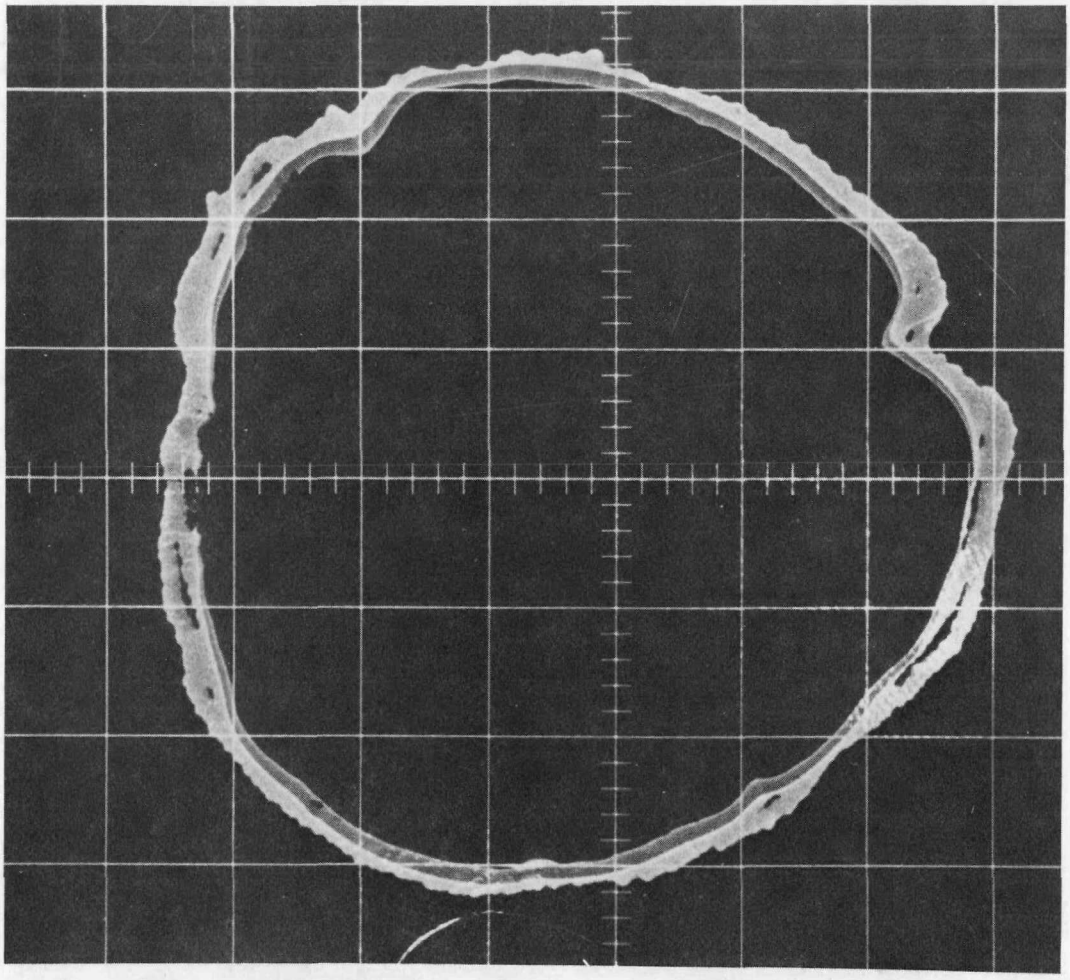

Figure 33. TYPICAL LISSAJOUS PATTERN OF RADIAL RUNOUT. (Total Indicated Runout of Eight Microinches. Scale: Ten Microinches per Centimeter)

y the spindle deflection as a function of time.

A_2, A_1, and A_0 are the characteristic constants.

With all initial conditions zero, the solution is:

$$Y(t) = \frac{F \exp\left(-\frac{A_1 t}{2A_2}\right) \sin\left[\sqrt{\frac{A_0}{A_2} - \left(\frac{A_1}{2A_2}\right)^2}\right] t}{A_2 \sqrt{\frac{A_0}{A_2} - \left(\frac{A_1}{2A_2}\right)^2}}$$

A_0 can be determined from the static stiffness test and the other constants determined from the dynamic test.

The resultant differential equation which adequately describes the spindle dynamic behavior is:

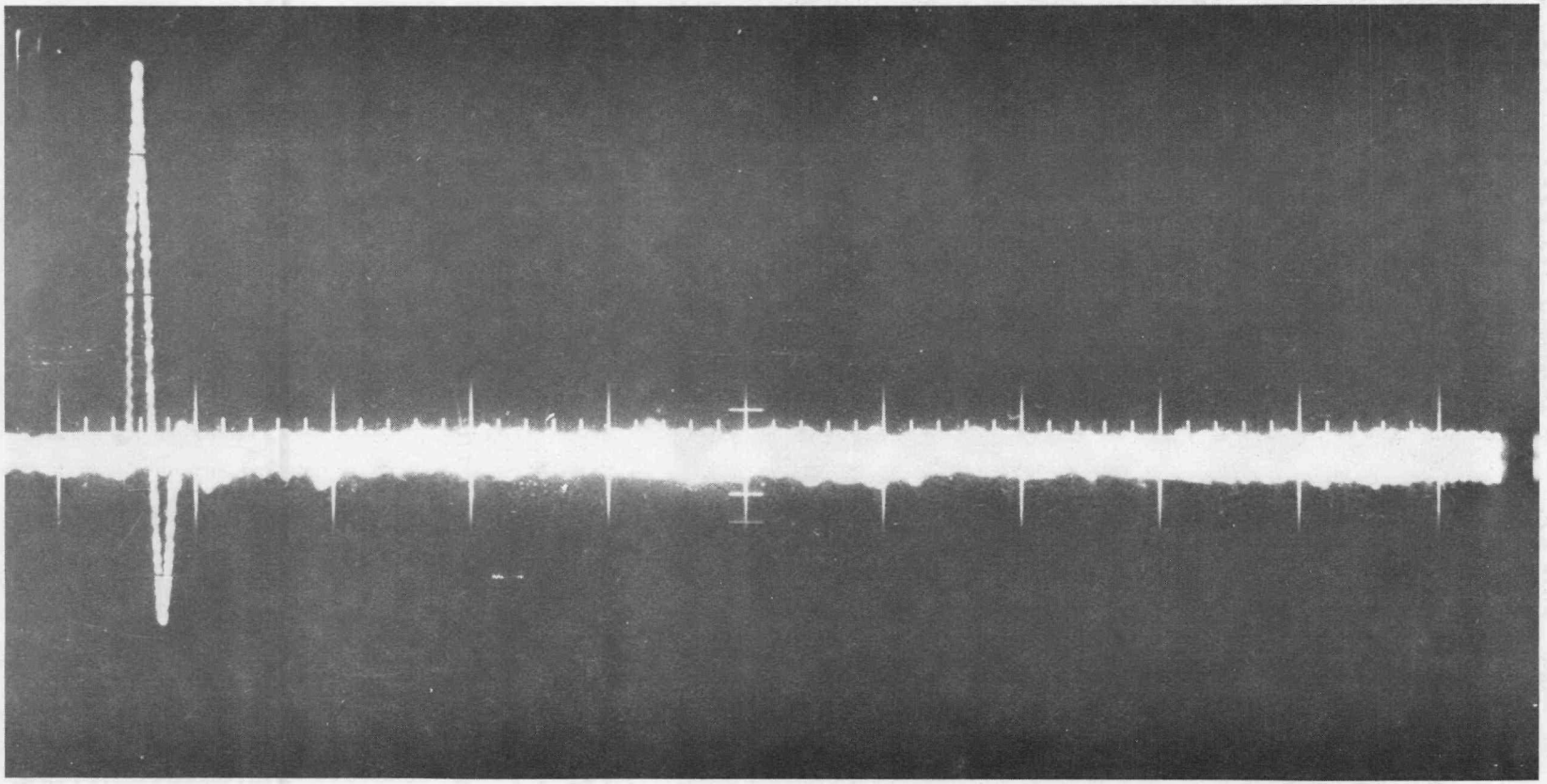

Figure 34. SPINDLE DEFLECTION RESPONSE TO AN APPLIED IMPULSE FORCE. (Sweep Rate - 20 Milliseconds per Centimeter)

$$1.8\frac{d^2y}{dt^2} + 1500\frac{dy}{dt} + 2.3 \times 10^6 y = f(t).$$

From these coefficients, the calculated damping factor is 0.5 and the resonant frequency is 167 cycles per second (cps), which means that if the spindle is excited with an abrupt change of force, such as occurs when cutting a part containing a sharp-edged hole or slot, the spindle deflection will be a maximum of 17% more than the same static deflection that would occur if the force was applied gradually. Based on the stiffness of the spindle measured at the face, initial deflection would be 0.51 microinch (13 nm) for each pound (4.4 N) of tool force applied. This deflection will settle out to the static value of 0.43 microinch (11 nm) in approximately one cycle, or 0.005 second. For instance, if the part is running at a surface speed of 600 ft/min (182 m/s), the transient deflection will settle out to the static value in 0.6 inch (15.2 mm) of part surface. In other words, chatter marks could be expected for 0.6 inch (15.2 mm) behind the hole, but the maximum depth would only be 0.10 microinch (2.5 nm) per pound (4.4 N) of tool force. In terms of a finish part cutting force of 20 pounds (88 N), this would amount to approximately 2 microinches (50.8 nm) maximum chatter depth. Results of this test indicate that the dynamic effects of the spindle deflection will be negligible for production applications since the step input function would be the most severe case encountered.

A second test was made on the spindle using a sinusoidal force input. The change in deflection, measured from the static rate for frequencies up to 50 cps, was negligible, which is in agreement with that predicted by the derived equation.

The performance measurements were made with the spindle operating on a 90-psig (620-kPa) supply of instrument air, film pressures of 58 - 64 psig (400 - 441 kPa) measured at the midpoint of the bearing, and a film thickness of approximately 300 microinches (7.6 μm).

The measured power consumption of the spindle at 2000 rpm was 0.5 horsepower (372 W); at 1000 rpm it was less than 0.15 horsepower (112 W). These values are in agreement with the calculated power consumption in the bearings. The overall mass of the spindle is about 800 pounds (363 kg). Such design modifications as a ribbed cast housing and additional paring of material at noncritical points could reduce this weight, if necessary, by several hundred pounds.

The reliability which can be expected from the porous graphite bearing design was clearly indicated through some mishaps which occurred during the performance tests. (Several mishaps happened during the testing of the cylindrical bearing design and one occurred to one of three spindles fabricated of the spherical design.) While testing the spherical bearing at 2200 rpm, the 300-pound (136-kg) rotor with a 200-pound (91-kg) part load suddenly seized in the front spherical bearing and stopped—all in a matter of a few seconds. Inspection of the spindle indicated that the journal had rubbed on a 1/4-inch (6.35-mm) band at the 80-degree portion of the bearing. A highly polished graphite surface and a slightly discolored 1/4-inch (6.35-mm)-wide band around the journal were the only effects that were observed after the mishap. The bearing was relapped and subsequent testing indicated that there was no change in performance. The relapping took about a half hour, then an hour or so was needed for disassembly and reassembly. The apparent cause of the seizure was from insufficient clearance at the 80-degree portion of the hemispherical bearing. This condition came about from the use of the wrong grade of lapping compound. After relapping with the proper finishing grade, no difficulty was encountered during the remaining spindle performance tests. All experience to date indicates that rubbing due to

short-term high loading, loss of air, or contaminant infiltration will not adversely affect spindle performance.

PREVENTATIVE MAINTENANCE

Very little preventative maintenance on an air-bearing spindle is required after the initial installation. Trouble-free performance for years can be realized with only a few precautions. A reasonably dry, oil-free, well-filtered air supply is required for the spindle bearings. Instrument air, final filtered with a 0.15-micrometre filter, was used for these spindles. This degree of filtration is required to prevent the microscopic pores of the graphite material from becoming plugged, which primarily range in diameter from 1.5 to 3.0 micrometres.

The air should be left on at all times to maintain the sealing action of the air escaping from the bearings. If possible, a pressure switch should be installed in the air-supply line to cut off the power to the spindle motor if the air pressure drops below a safe operating level [usually 70 psig (483 kPa)]. Care should also be taken to insure that the spindle is not overloaded.

REPAIR

In the event of a bearing failure, steps must be taken to restore the bearing to operation. First step in the rework procedure is to ascertain why the bearing failed and to take steps to prevent a recurring failure. Air bearings can fail for any of the following reasons:

1. Improper adjustment. A proper preload and distance between the bearing pad and journal are essential.

2. The porous graphite restriction material has become clogged by oil. Oil can enter the bearing either through the air supply line or through the opening to the outside when the air supply is off.

3. Dirt or dust has entered the bearing by the same routes as the oil previously mentioned.

4. The supply pressure has pushed the graphite bearing material away from the metal housing, breaking the epoxy bond between the two.

Guidelines for restoring the bearing for each case just listed are as follows (each restoration number corresponds to the number for each type of failure):

1. Readjust to obtain proper clearances and film pressures according to the manufacturer's directions.

2. Install proper filters in the air supply line. Filters are commercially available which remove oil, water, and particles down to 0.15 micrometre. Flush the bearing by pumping solvent through the air supply lines. Trichloroethylene is an acceptable solvent. Do not use methylene chloride for flushing the bearings as this solvent will soften the epoxy bonding the graphite to the metal housing. Relap bearings and/or journals if their surfaces are damaged. Impregnate graphite to obtain proper restriction.

3. Same guidelines as for Failure 2.

4. Measure the surface with an indicator to determine the extent of the area blown loose (Figure 35). If damage is not over 20 - 30% of the area, the bearing may be repaired by fastening the blown-out portion to the housing by flat-head screws (Figure 36). However, this method may lead to somewhat less than optimum stiffness and pneumatic instability resistance. If damage is extensive, the liner should be replaced, relapped, and reimpregnated. Specific procedures for lapping both journals and graphite bearings of a spherical spindle have been included in the section on FABRICATION.

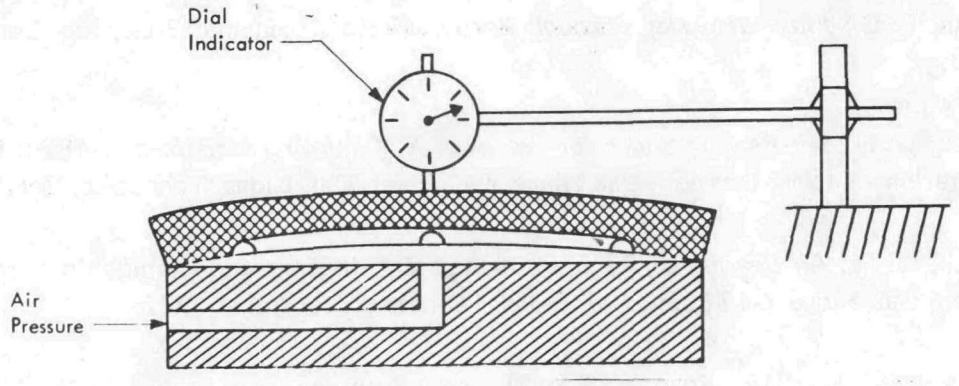

Figure 35. MEASURING FOR BLOWN LOOSE GRAPHITE.

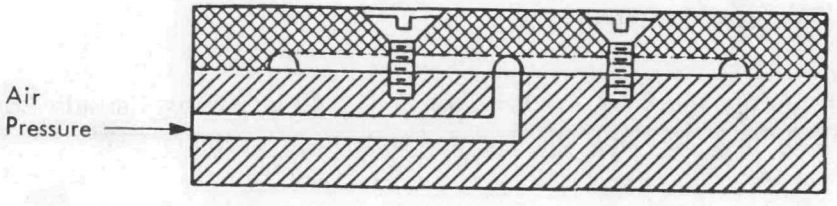

Figure 36. REPAIR OF BLOWN LOOSE GRAPHITE.

BIBILOGRAPHY

Steger, P. J. and Abbatiello, L. A.; *Air-Bearing Spindles for Production Machine Tools,* Y-1578; Union Carbide Corporation—Nuclear Division, Oak Ridge Y-12 Plant, Oak Ridge, Tennessee; September 25, 1967.

Steger, P. J.; *Air-Bearing Spindle for Machine Tools - Spherical Design,* Y-1581; Union Carbide Corporation—Nuclear Division, Oak Ridge Y-12 Plant, Oak Ridge, Tennessee; September 29, 1967.

Shell, M. L. and Steger, P. J.; *Air-Bearing Steady Rest for Production Machine Tools,* Y-SC-4; Union Carbide Corporation—Nuclear Division, Oak Ridge Y-12 Plant, Oak Ridge, Tennessee; March 25, 1970.

Woodall, N. D; *Application of Air Bearings and Laser Interferometry to an Inspection Machine,* 70-WA/Prod-29; ASME Winter Annual Meeting, New York, New York; November 29-December 3, 1970.

Rasnick, W. H. and Shell, M. L.; *Impregnation of Porous Graphite for Flow Modification,* Y-SC-7; Union Carbide Corporation—Nuclear Division, Oak Ridge Y-12 Plant, Oak Ridge, Tennessee; June 1971.

Fuller, D. C.; *Theory and Practice of Lubrication for Engineers;* John Wiley and Sons, Inc, New York, New York (1956).

Carman, P. C.; *Flow of Gases Through Porous Media;* Academic Press, Inc, London, England (1956).

Rasnick, W. H.; *Air-Bearing Slides for Precision X-Y Turning Machines,* Y-1824; Union Carbide Corporation—Nuclear Division, Oak Ridge Y-12 Plant, Oak Ridge, Tennessee; March 1972.

Rasnick, W. H.; *Air-Bearing L VDT Transducer,* Y-DA-4839; Union Carbide Corporation—Nuclear Division, Oak Ridge Y-12 Plant, Oak Ridge, Tennessee; November 1972.

Rasnick, W. H.; *Air Bearing Rework and Impregnation,* Y-DA-4838; Union Carbide Corporation—Nuclear Division, Oak Ridge Y-12 Plant, Oak Ridge, Tennessee; November 1972.

Steger, P. J.; *Practical Design Considerations for the Application of Gas Bearings to Machining Processes,* Y-DA-4541; Union Carbide Corporation—Nuclear Division, Oak Ridge Y-12 Plant, Oak Ridge, Tennessee; September 1972.

Steger, P. J.; *Applications of Air Bearings,* Y-DA-4834; Union Carbide Corporation—Nuclear Division, Oak Ridge Y-12 Plant, Oak Ridge, Tennessee; November 1972.

Steger, P. J.; *Spindle Evaluation*, Y-DA-4833; Union Carbide Corporation—Nuclear Division, Oak Ridge Y-12 Plant, Oak Ridge, Tennessee; November 1972.

NOTATION*

A	Projected area (in^2)
a,c,l	Length dimension as noted (in)
A_s	Surface area (in^2)
b	Bearing perimeter (in)
E	Modulus of elasticity (lbs/in^2)
E_f	Bearing geometry factor
F	Tool force, axial (lbs)
h	Film thickness (in)
I	Moment of inertia (in^4)
J	778 (ft lbs/Btu)
K	Spring constant (lbs/in)
L	Shaft length between bearings (in)
k	Permeability (in^2)
l_s	Slot length (in)
M	Friction moment (in/lb)
N	Shaft speed (rpm)
P	Pressure (lbs/in^2)
q	Heat generation (Btu/sec)
Q	Volumetric gas flow (in^3 sec)
R	Reaction force (lbs)
r	Radius of spherical zone (in)
S	Bearing film stiffness (lbs/in)
ΔT	Temperature (^{o} F)
t	Material thickness (in)
V	Surface velocity (in/sec)
W	Tool force, radial (lbs)
y,Δs,Δw	Deflection (in)
a	Thermal coefficient of expansion (in/in-^{o} F)
δ	Thermal growth (in)
μ	Viscosity (lb-sec/in^2)

*Unless specifically defined in text.

APPENDIX

SAMPLE DESIGN CALCULATION FOR A SIX-INCH-RADIUS SPHERICAL-ZONE SPINDLE

Design conditions:

1. Load capacity, 500 lbs (6" from spindle face).

2. Deflection: radial (2 μin/lb 6" from spindle face); axial (2 μin/lb).

3. Supply pressure = 80 psig.

Once design conditions have been established, it is best to simply draw an approximate design and run through the calculations to decide whether or not it meets the design criteria. In this particular case, start with a 6-inch-radius spindle with an 8-inch-diameter shaft that is 18 inches long between bearing centers. (Figure A-1)

B_1 should be set at a few degrees more than 0°. In this case, choose 5°. B_2 can be calculated by $B_2 = \cos^{-1}(4/6) - 47°$.

The bearing geometry efficiency factor can now be calculated:

$$E_f = \frac{(\sin B - \sin^3 B)\Big]_{\frac{5\pi}{180}}^{\frac{47\pi}{180}} \left(\frac{\theta}{2} + \frac{\sin 2\theta}{4}\right)\Big]_{\frac{-\pi}{2}}^{\frac{\pi}{2}}}{\left(\frac{B}{2} + \frac{\sin 2B}{4}\right)\Big]_{\frac{5\pi}{180}}^{\frac{47\pi}{180}} (\sin\theta)\Big]_{\frac{-\pi}{2}}^{\frac{\pi}{2}}}, \text{ or}$$

$$E_f = \frac{[(0.731 - 0.130) - (0.087 - 0.0007)]\ [(0.785 + 0) - (-0.785 + 0)]}{[(0.410 + 0.249) - (0.087 + 0.043)]\ [(1) - (-1)]}, \text{ or}$$

$$E_f = \frac{[0.514]\ [1.57]}{[0.529]\ [2]}, \text{ or}$$

$E_f = 0.762$.

Choosing h = 300 μin,

static bearing film stiffness is:

$$S = E_f \frac{0.35\ Ps}{h}, \text{ or}$$

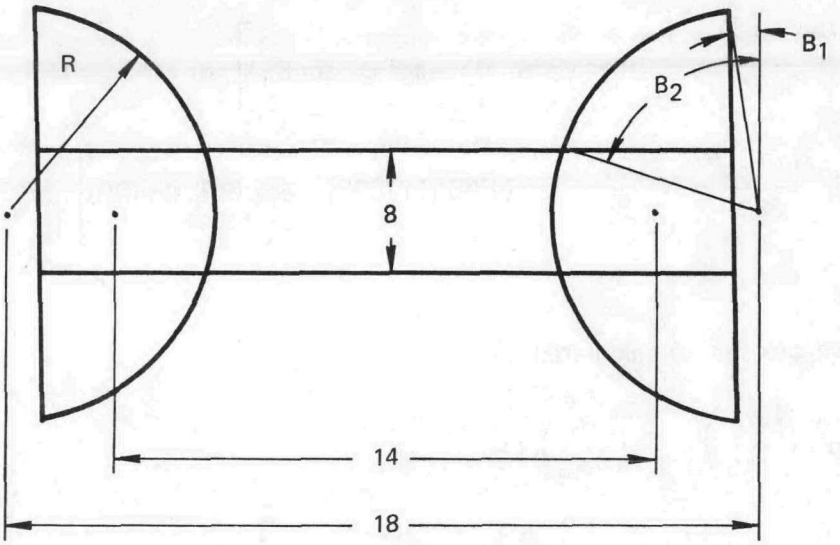

Figure A-1. SPINDLE AND SHAFT.

$$S = \frac{(0.762)\ (0.35)\ (80\ lb/in^2)}{300 \times 10^{-6}\ in}, \text{ or}$$

$S = 71{,}120\ lb/in/in^2$ area.

Using the free-body diagrams in Figure 11, the reaction forces at the front and rear bearings can be calculated:

$L = 18 - 4 = 14,$

$c = 6 + 2 = 8.$

Assuming 1 lb of force and summing the forces and moments:

$R_f + R_r + w = 0,$

$L\ (R_f) + L + c\ (w) = 0,$

$14\ (R_f) = 22\ (w),$

$$R_f = \frac{22}{14}\ (w) = 1.57\ lb, \text{ or}$$

$R_r = 1 - 1.57,$ or

$R_r = -\ 0.57$ lb (- sign denotes direction).

Projected area for bearing:

$$= 2\left[\pi R_2 \frac{(B_2 - B_1)}{360} + \frac{R_2}{2}(\cos B_2 \sin B_2 - \cos B_1 \sin B_1)\right], \text{ or}$$

$$= 2\left[\pi(6)^2 \frac{(47^o - 5^o)}{360^o} + \frac{(6)^2}{2} \cos(47^o) \sin(47^o) - \cos(5^o) \sin(5^o)\right], \text{ or}$$

$= 41.23 \text{ in}^2$.

Film deflections can be calculated by:

$$\Delta w = \frac{L + c}{L}\left(\frac{R_f}{2AS}\right) + \frac{c}{L}\left(\frac{R_r}{2AS}\right), \text{ or}$$

$$\Delta w = \frac{14 + 8}{14}\left[\frac{1.57}{2\ (41.2)\ (71{,}000)}\right] + \frac{8}{14}\left[\frac{0.57}{2\ (41.2)\ (71{,}000)}\right], \text{or}$$

$\Delta w = 0.42 \times 10^{-6} + 0.06 \times 10^{-6} = 0.48 \times 10^{-6}$ in.

Shaft deflection due to bending can be determined by the following equations:

$$Y_{(a)} \text{ (deflection at } \underline{a}) = \frac{Wa}{2EI}\left(ca - \frac{a^2}{3} + \frac{2cL}{3}\right)$$

$$I = \frac{\pi r^4}{4} = \frac{\pi(6)^4}{4} = 1017$$

$$Y_{(a)} = \frac{(1)\ (8)}{2(30 \times 10^6)\ (1017)}\left[(64) - \frac{64}{3} + \frac{2}{3}(8)\ (14)\right]$$

$Y_{(a)} = 0.015 \times 10^{-6}$ in.

$$Y'_{(a)} = \frac{W}{EI}\left(ca - \frac{a^2}{2} + \frac{cL}{3}\right), \text{ or}$$

$Y'_{(a)} = 0.002 \times 10^6$.

$\Delta s = Y_{(a)} + (c - a)\ Y'_{(a)}$, or

$= 0.015 \times 10^{-6} + (0)Y'$, or

$= 0.015 \times 10^{-6}$ in/lb.

Total radial deflection:

$= \Delta w + \Delta s$, or

$= 0.48 \times 10^{-6} + 0.015 \times 10^{-6}$, or

$= 0.50 \times 10^{-6}$ in/lb.

Axial deflection:

Projected Area $= \pi(R_o^2 - R_i^2) = \pi\{[6(\cos 5^o)]^2 - [6(\cos 47^o)^2]\}$, or

$= \pi(35.7 - 16.74)$, or

$= 59.5$ in^2.

$$\Delta_a = \frac{F}{A(S)}, \text{ or}$$

$$\Delta_a = \frac{1}{(59.5)\ (71{,}000)}, \text{ or}$$

$\Delta_a = 0.24 \times 10^{-6}$ in/lb.

Load capacity (axial):

Let $\Delta_a = 150 \times 10^{-6}$, then

solve for F:

$(150 \times 10^{-6})\ (59.5)\ (71{,}000) = F$, or

F = 634 lb.

Load capacity (radial):

The front bearing carries 1.57 times the load at 6 inches from the face:

$$\Delta f = 150 \times 10^{-6}\ \mu\text{inch} = \frac{1.57\ F}{2\ \ (41.2)\ (71{,}000)}, \text{ or}$$

F = 559 lb.

Comparing design calculations with conditions yields:

	Conditional Value	Calculated Value
Load Capacity	500 lbs, 6 in from face	559 lbs, 6 in from face
Deflection		
Radial	2 μin/lb	0.50 μin/lb
Axial	2 μin/lb	0.24 μin/lb

Heat generated at 1500 rpm can be calculated by:

$$q = \frac{2\pi MN}{720J},$$

where $M = \frac{\mu r A_s V}{h}$.

For a spherical zone bearing:

$$M = \frac{0.66\, N\mu r^4}{h} \int_{B_1 = 5^o}^{B_2 = 47^o} \sin^4 B dB$$

$$A_s = \frac{47 - 5}{360}(4\pi r^2) = 52.8 \text{ in}^2$$

$$M = \frac{(0.66)\ (1500)\ (0.026 \times 10^{-7})\ (1296)}{3 \times 10^{-4}}\ 0.5\ , \text{ or}$$

M = 5.5 in lb.

$$q = \frac{(2\pi)\ (5.5)\ (1500)}{720\ (778)}, \text{ or}$$

q = 0.09 Btu/sec per bearing.

The air flow through the bearings is determined by:

$$Q_a = \frac{bh^3}{24\mu l_s P_f}\ (P_f^2 - P_a^2),$$

where b represents the perimeter.

$b_o = 2\ \pi \times 6 \times (\cos 5^o) + 2\pi \times 6 \times (\cos 47^o)$.

If the bearing is segmented in quadrants:

$$b = b_o + 8 \times \frac{(47^o - 5^o)}{360} \times 2\pi \times 6, \text{ or}$$

b = 63 + 35, or

$b = 98.2$ in.

$l_s = 1.6 \times 10^3 \, p^{0.6} h^{1.4}$.

Let film pressure = 45 psig, then:

$l_s = (1.6 \times 10^3)\,(45)^{0.6}\,(3 \times 10^{-4})^{1.4}$, or

$l_s = 0.190$ in.

$$Q_a = \frac{(98.2)\,(0.0003)^3\,(60^2 - 15^2)}{24\,(0.026 \times 10^{-7})\,(0.19)\,(60 \text{ psia})}, \text{ or}$$

$Q_a = 12.6$ in^3/sec.

Equating this flow with Darcy's law and letting the graphite thickness be 0.5 inch yields:

$$\frac{KA_s\,(95^2 - 60^2)}{2\mu T60} = \frac{K(52.8)\,(95^2 - 60^2)}{2(0.026 \times 10^{-7})\,(0.5)\,(60)} = K\ 1.83 \times 10^{12}, \text{ or}$$

$$12.6 = K(1.836) \times 10^{12} \text{ or}$$

$$K = 6.86 \times 10^{-12}.$$

This is the required permeability of the graphite. Darcy's equation can be used to calculate the flow required for impregnation. For example, if a two-inch-diameter probe is available, and if the supply pressure is set at 40 psig (or 55 psia), then the flowmeter reading can be calculated:

$$Q = \frac{KA\left(P_1^2 - P_2^2\right)}{2\mu T P_2}, \text{ or}$$

$$Q = \frac{(6.86 \times 10^{-12})\left(\frac{\pi 2^2}{4}\right)(55^2 - 15^2)}{2\,(0.026 \times 10^{-7})\,(0.5)\,(15)}, \text{ or}$$

$Q = 1.55$ in^3/sec.

ENDORSEMENT NOTICE

REFERENCE TO A COMPANY OR PRODUCT NAME DOES NOT IMPLY APPROVAL OR RECOMMENDATION OF THE PRODUCT BY UNION CARBIDE CORPORATION OR THE U. S. ATOMIC ENERGY COMMISSION

NOTICE